CORAL ISOTOPE RECORD OF ENVIRONMENTAL CHANGE IN THE NORTHWEST GULF OF MEXICO

A Thesis

by

ADRIAN MINER

Submitted to the Office of Graduate and Professional Studies of
Texas A&M University
in partial fulfillment of the requirements for the degree of

MASTER OF SCIENCE

Chair of Committee,	Niall C. Slowey
Committee Members,	Deborah J. Thomas
	Matthew W. Schmidt
Head of Department,	Piers Chapman

December 2013

Major Subject: Oceanography

ABSTRACT

Variations in the density banding and chemical composition of the skeletal material of long-lived corals in the Gulf of Mexico preserve records of past environmental conditions. To better interpret these records, the controlling mechanisms governing carbon and oxygen isotopes in coral skeletal material must be well understood. We have studied a *Montastrea faveolata* coral core from the Flower Garden Banks deposited over the 161 year period from 1844 to 2005. Annual growth bands revealed by X-radiography indicate the years and rates at which this material was deposited. We used a micro-milling device to obtain calcium carbonate samples at increments corresponding to approximately monthly resolution, and measured their stable oxygen ($\delta^{18}O$) and carbon isotope ($\delta^{13}C$) ratios with a mass spectrometer. The stable isotope records from this *Montastrea faveolata* coral reflect differences in the environmental controls of $\delta^{18}O$ and $\delta^{13}C$ fractionation. Annual variations of $\delta^{18}O$ coincide with density bands and reflect changes of seawater temperature, which in turn are linked to climate. Annual variations of $\delta^{13}C$, which are largely controlled by photosynthesis, coincide with changes of insolation. Changes in the annual cycle of $\delta^{18}O$ lag those of $\delta^{13}C$ by about 2 months. We propose this difference exists because at the Flower Garden Banks the response of photosynthesis to seasonal changes in insolation occurs more rapidly than that of seawater temperature. Over the 161 year period of the record, the overall trend of $\delta^{13}C$ is toward more negative values and the annual range of $\delta^{13}C$ values increases. These patterns are consistent with the flux of fossil-fuel-derived

carbon dioxide from the atmosphere to the ocean. Within the period of about 1900 to 1920, several years display particularly negative values. We speculate these values may result from Northern Hemisphere volcanism and/or interannual climate fluctuations.

DEDICATION

This work is dedicated to my mom and dad. I couldn't have asked for better parents.

ACKNOWLEDGEMENTS

First and foremost, I would like to thank Niall Slowey for his guidance throughout my thesis research. After my father, Niall has been the most important role model in my life. The lessons I have learned under him have helped me become a better scientist; and more importantly, a better person. I am glad to have come to Texas A&M and grateful to be able to call Niall a friend. I would also like to thank Matthew Schmidt and Debbie Thomas, who have offered advice on my thesis research, helped me develop my knowledge of paleoceanography, and supported me in other times of need.

I would also like to thank Bill Bryant and Stuart Burbach for their kindness and generosity. The geological problems we worked on together were fun and engaging, and it was an honor just to be around both of them. The numerous ways they helped me during the final days of my thesis work made it possible for me to accomplish my goals and I will never forget that.

Mom and Dad, your love and support have always been constant and were essential during the highs and lows of my thesis research. I have come to gain a greater appreciation for the quality and strength of our family after moving thousands of miles away from home. I am profoundly grateful to have you as parents.

Teddy, you are a good friend and confidant. There are a very few people in my life to whom I have become close enough to gain a deep appreciation of their true strengths. I gained a great deal in our friendship and without your help, I am not sure I

would have learned as much as I have during the last four years. I wish you the best in all your endeavors.

My love and gratitude to everyone I have had the chance to work with and befriend during my time at Texas A&M. I learned important lessons from you and you have my admiration; and with that, I feel confident and prepared for what comes next.

My graduate studies and this project were made possible by support from the Norman Hackerman Advanced Research Program, the NOAA Flower Gardens Banks National Marine Sanctuary, and the National Science Foundation S-STEM Graduate Fellowship program.

NOMENCLATURE

$\delta^{13}C$	^{13}C to ^{12}C Isotope Ratio
$\delta^{18}O$	^{18}O to ^{16}O Isotope Ratio
$\Delta^{14}C$	Measure of ^{14}C Abundance Relative to Stable C Isotopes
µg	Micrograms
‰	Per mille
^{o}C	Degrees Celsius
CO_2	Carbon Dioxide
DIC	Dissolved Inorganic Carbon
ENSO	El Niño-Southern Oscillation
m	Meters
mm	Millimeters
PNA	Pacific/North American
ppm	Parts per million
P/R	Photosynthesis/Respiration
PSU	Practical Salinity Units
Sr/Ca	Strontium/Calcium Ratio
SST	Sea Surface Temperature

TABLE OF CONTENTS

LIST OF FIGURES

Page

LIST OF TABLES

1. INTRODUCTION

Changes in the stable isotopic composition of coral skeletal material provide invaluable information about past environmental conditions. Most previous studies have focused on variations of oxygen isotopes, which yield quantitative information about variations of the temperature and salinity of seawater [e.g., *Weber and Woodhead*, 1970; *Dunbar and Wellington*, 1981; *Weil et al*., 1981; *Cole et al*., 1993; *Dunbar et al*., 1994]. Knowledge of these fundamental parameters has lead to significant insight into the temporal character of past oceanographic and climatic conditions [e.g., *Shen et al*., 1992; *Cole et al*., 1993; *Cobb et al*., 2003]. The amount of oxygen isotope records is equaled by the amount of carbon isotope records. Yet, while some studies have also considered variations in the carbon isotopic compositions of corals [e.g., *Weber and Woodhead*, 1970; *Land et al.,* 1975; *Goreau*, 1977; *Fairbanks and Dodge*, 1979; *McConnaughey*, 1989a,b; *Gagan et al*., 1996; *Swart et al.,* 1996; *Grottoli and Wellington*, 1999], much less attention has been paid to these records because their relationship to environmental conditions is less certain. Improved understanding of the environmental controls of coral carbon isotope ratios will make it possible to interpret carbon isotope records from long-lived corals in terms of past oceanographic and climatic conditions.

Seasonal fluctuations of climate strongly influence environmental conditions in the northern Gulf of Mexico. Insolation varies annually from about 275 to 435 W/m^2 due to variations in the position of the Earth's axis relative to the ecliptic plane [e.g., *Berger*, 1979], with additional effects due to variations of cloud cover in conjunction with interannual climate variations [e.g., *Hansen*, 1971; *Reed*, 1977]. While subtropical

conditions exist during summer, the passage of fronts can bring very cold Arctic air to the region [e.g., *Erhardt*, 1990; *Rogers and Rohli*, 1991]. For this reason, winter temperatures along the gulf coast can be quite cold, and the average winter temperature has varied as much as 8 °C over the last several decades [e.g., *Erhardt*, 1990; *Leathers et al*., 1991]. The variations in cloudiness and temperature reflect broad-scale fluctuations in the winter climate of North America that also affect the Gulf of Mexico [*Nowlin and Parker,* 1974; *Slowey and Crowley, 1995*]. Furthermore, the upper ocean carbon reservoir in the Gulf of Mexico is likely to have been altered by long-term changes in atmospheric CO_2 due to anthropogenic forcing, as has been observed elsewhere [*Sabine et al.,* 2004, *Gledhill et al.,* 2008; *Swart et al.,* 2010]. Unfortunately, our knowledge of how environmental conditions in the Gulf of Mexico have varied over time, the influence of such variations on marine organisms, and their implications for our understanding of the climate of North America is limited. The research presented here improves understanding of these areas through the investigation of corals that live at the Flower Garden Banks and the environmental information they preserve.

Factors such as photosynthesis and respiration, water depth, the dissolved inorganic carbon (DIC) of ambient seawater, extension rate, eutrophy, and spawning have all been considered as controls on annual carbon isotope cycles recorded in coral skeletons [e.g., *Weber and Woodhead*, 1970; *Land et al.,* 1974; *Goreau*, 1977; *Fairbanks and Dodge*, 1979; *McConnaughey*, 1989a,b; *Gagan et al*., 1996; *Swart et al.,* 1996; *Grottoli and Wellington*, 1999]. Our record provides unique insights into the relative importance of each controlling factor for carbon isotopes in *M. faveolata* because the

environment from which the coral selected for this study was extracted differs in important ways from the environments of past coral studies [e.g., *Fairbanks and Dodge*, 1979; *Shen et al*., 1992; *Cole et al*., 1993; *Swart et al*., 1996; *Linsley et al*., 2000]. The coral core selected for this project was extracted from the West Flower Garden Banks, an open ocean environment and at remarkable water depths below the sea surface. As a result, carbon isotopes behave in ways that more readily reveal their controlling environmental factors.

The East and West Flower Garden Banks are located approximately 185 km offshore of Galveston, Texas at the edge of the broad Texas-Louisiana Continental Shelf (Figure 1). The banks are situated atop salt domes generated by the upward flowage of salt through overlying sediments [e.g., *Humphris*, 1979, *Peel et al.,* 1995]. The West Flower Garden Bank rises from the surrounding seafloor depth of 120 meters to within 20 meters of the sea surface at its apex [*Levert and Ferguson*, 1969]. The high bathymetry and hard rock substrate of the West Flower Gardens Bank support the growth of the most northerly-located hermatypic coral reefs on the North American continent [*Rezak et al.,* 1985; *Hagman and Gittings*, 1992]. Corals living at the crests of the banks grow at depths of 20 to 22 m below the sea surface [*Rezak et al.*, 1985] where the observed annual ranges of seawater temperature, salinity and oxygen isotopic composition correspond to open-ocean conditions [*Rezak et al.,* 1985; *Hagman and Gittings*, 1992; *Antonov et al*., 1996; *Wagner and Slowey*, 2011].

Carbon and oxygen isotopes from an individual coral head are inextricably linked to the environmental variables that were present when the coral was alive

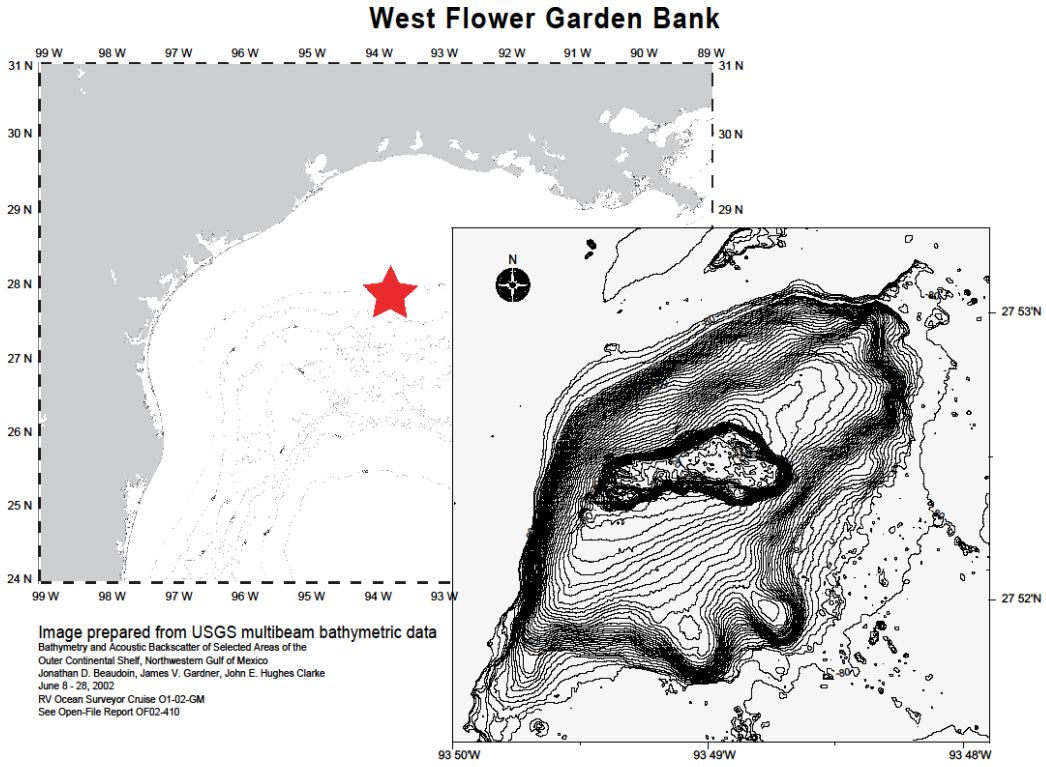

Figure 1. Study location: West Flower Garden Banks

[e.g., *Weber and Woodhead*, 1970; *Weber and Woodhead*, 1972; *Fairbanks and Dodge,* 1979; *Dunbar et al*., 1981; *Weil et al*., 1981]. Although this study is foremost an exercise in understanding the controlling factors on $\delta^{13}C$ variability, an acute understanding of $\delta^{18}O$ and the variables that affect it is required to fully appreciate carbon isotope mechanics and other coral physiological processes. In addition to the multiple isotope approach to understanding coral physiological processes, an investigation of coral density bands was conducted. Studies have shown *M. faveolata* corals exhibit variations in skeletal density thought to be associated with seasonal changes in environmental conditions resulting in the annual formation of high and low density bands [*Knutson and Smith*, 1972; *Dodge and Thomson*, 1974; *Hudson et al*., 1976] although some disagreement exists regarding the dominant controlling environmental factors affecting coral growth [e.g., *Knutson and Smith,* 1972; *Buddemeier and Kinszie*, 1976; *Hudson et al.,* 1976; *Hudson and Robbin*, 1980; *Dodge and Lang*, 1983; *Glynn and Wellington,* 1983]. On longer timescales, workers contend that measurement of extension rates and density banding in *Montastrea faveolata* at the Flower Garden Banks respond to and provide clues about long-term regional shifts in winter climate during the past several hundred years [*Slowey and Crowley,* 1995]. In this paper, we examine seasonal and interdecadal scale shifts in coral growth by coupling variations in the chemical composition of coral skeletons at the Flower Garden Banks to density variations in coral skeletons. Moreover, the marriage of geochemical data to coral extension measurements provided a direct method to link past environmental variables to coral growth.

The primary aim of the research presented in this thesis is to better understand how environmental conditions at the Flower Garden Banks affect the growth and isotope fractionation of *M. faveolata* corals, and in turn, how changes in these parameters record the history of environmental change in the northwest Gulf of Mexico. More specifically, we address longstanding questions about the controlling mechanisms on coral skeletal $\delta^{13}C$ and provide a case for the viability of $\delta^{13}C$ as a time marker for age. Furthermore, long term trends in carbon isotope variability were examined and provide insight into natural and anthropogenic forcing on carbon in the waters of the northwest Gulf of Mexico. A greater understanding of climatological variability and coral physiological process in the Gulf of Mexico was attained by constructing the longest extension band record from the Flower Garden Banks *M. faveolata* coral examined here.

2. CORAL CORE SAMPLES AND ANALYTICAL METHODS

In May of 2005, two long cores of coral skeletal material were collected from *M. faveolata* corals living at the West Flower Garden Bank using a hydraulic drill with 4-inch outer diameter diamond tipped drill bits [see *Wagner et al.*, 2011]. Cores were collected from the central region of the dome-shaped coral heads, where minimal variability of extension-rate related isotope disequilibria effects occur [e.g., *McConnaughey*, 1989a,b]. A custom-made saw fitted with two parallel diamond-coated circular blades at the Texas A&M Department of Oceanography was used to cut 8-mm-thick slabs of skeletal material from the longitudinal axis of each core section. To facilitate the measurement of coral extension rate and sampling of the slabs for stable isotope analysis, care was taken to cut each slab in an orientation that maximized the down core continuity of exposed corallite thecal walls. Each slab was then thoroughly cleaned with deionized water and dried.

X-radiographs of the coral slabs from the two coral cores revealed down core variations in coral density due to the presence of clearly recognizable annually-produced couplets of high and low density bands, with high-density corresponding to summertime, and other occasional thin and more-irregular high-density bands related to extreme winter stress due to low temperatures [e.g., *Buddemeier and Kinszie*, 1976; *Hudson et al.,* 1976]. X-radiograph images were then loaded into the *ImageJ* software package [*Schneider et al.,* 2012] which accurately calculated scale measurements of the coral slab and quantified the greyscale of each individual pixel, in turn, providing a direct high resolution measure of density down the coral core. Starting at the top of the coral core,

where the most recently deposited skeletal material was formed in early 2005, the greyscale variations measured by the *ImageJ* software package were counted and used to identify the year of deposition for successively older annual density bands. The X-radiographs were then examined for sampling potential, which included: direction of growth relative to the planar sampling surface, differentiation of stress bands from annual bands, the presence of annual bands, and the level of preservation of skeletal matter. West Flower Garden Bank core WFG2, which is 1.3-m long, was selected for detailed stable isotope analysis (Figure 2).

The samples for stable isotope analysis were collected from exposed coral thecal walls that parallel the axis of coral growth. This approach avoided isotope measurement variability related to differences in the composition of thecal wall and endothecal portions of the coral skeletal material, and it maximized the material obtained for each sample since the thecal wall is the densest portion of the coral chalice [*Patzold,* 1984; *Patzold*, 1992; *Leder et al*., 1996]. Coral sampling was conducted using a computer-aided triaxial-micromilling device with a 0.5-mm-diameter diamond-coated dental drill bit and custom built rotating stage. Each coral slab was mounted to the rotating stage, which made it possible to easily adjust the coral slab's orientation whenever a change in the direction of the coral thecal wall path was encountered.

In all, 498 coral samples were isotopically analyzed to determine an optimal sampling strategy. Three transects were sampled side-by-side at 1.0-mm width by 0.5-mm intervals down the growth axis of the examined *M. faveolata* coral core. In each

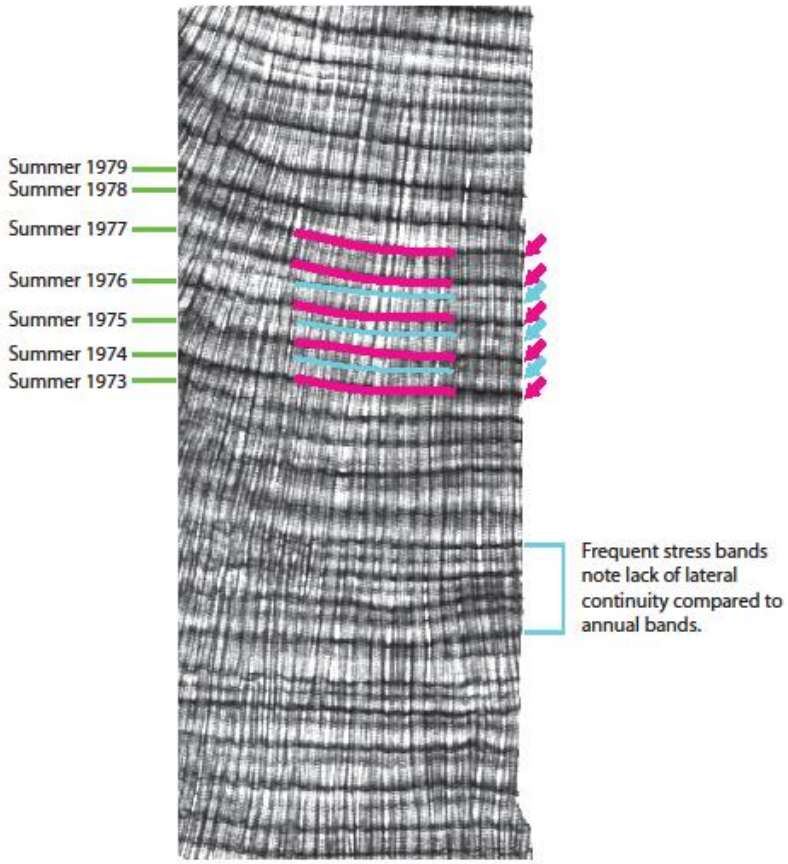

Figure 2. An X-radiograph of *Montastrea faveolata* coral slab used in this study. Lighter bands represent less dense coral skeletal material that was deposited during wintertime months and darker bands represent higher density skeletal material that is typically deposited during summertime months. Thinner dark bands that bisect winter low density bands are winter stress bands deposited when the coral is stressed by low temperatures.

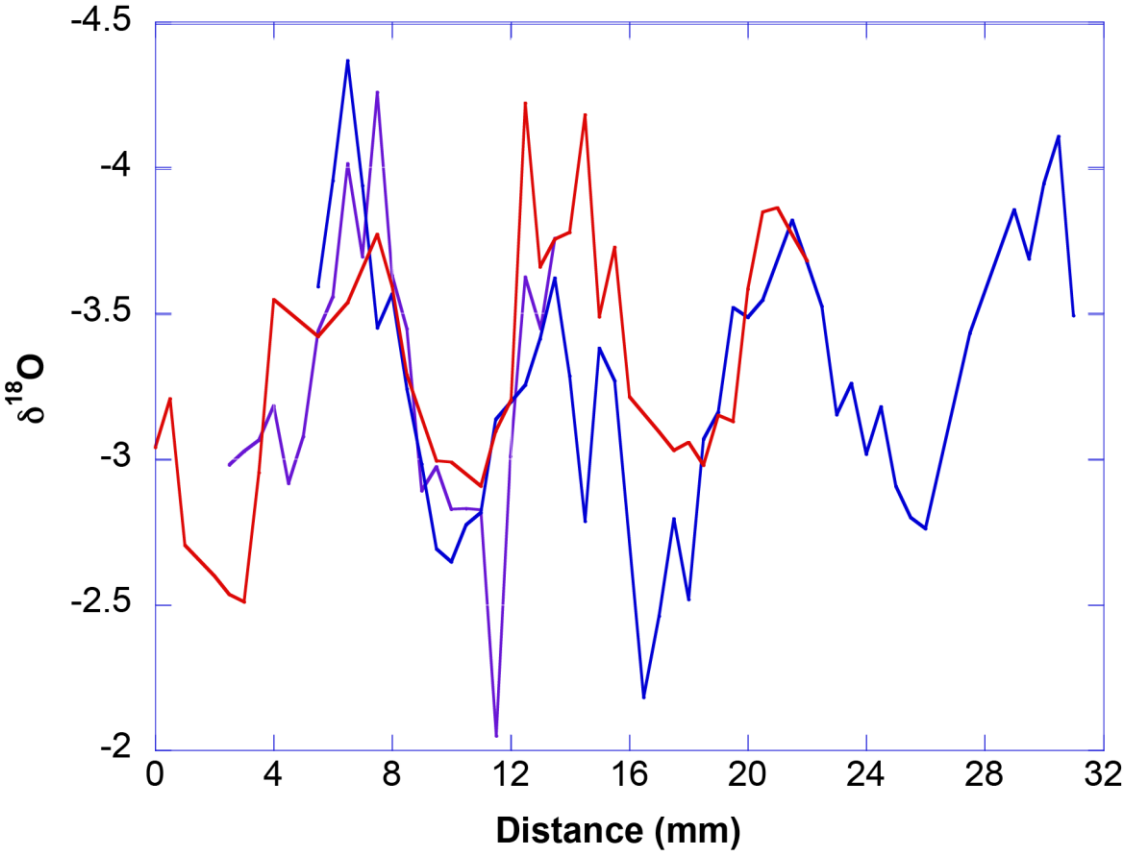

Figure 3a. Flower Garden Banks *M. faveolata* $\delta^{18}O$ values corresponding to 1.0-mm wide x 0.5-mm long x (N)-mm deep sampling strategy sampled at (Green) 0.34-mm depth, (Blue) 0.5-mm depth, and (Red) 0.67-mm depth. There is little difference between each sampling strategy although 0.34-mm and 0.5-mm depth drill cuts show almost no summertime difference.

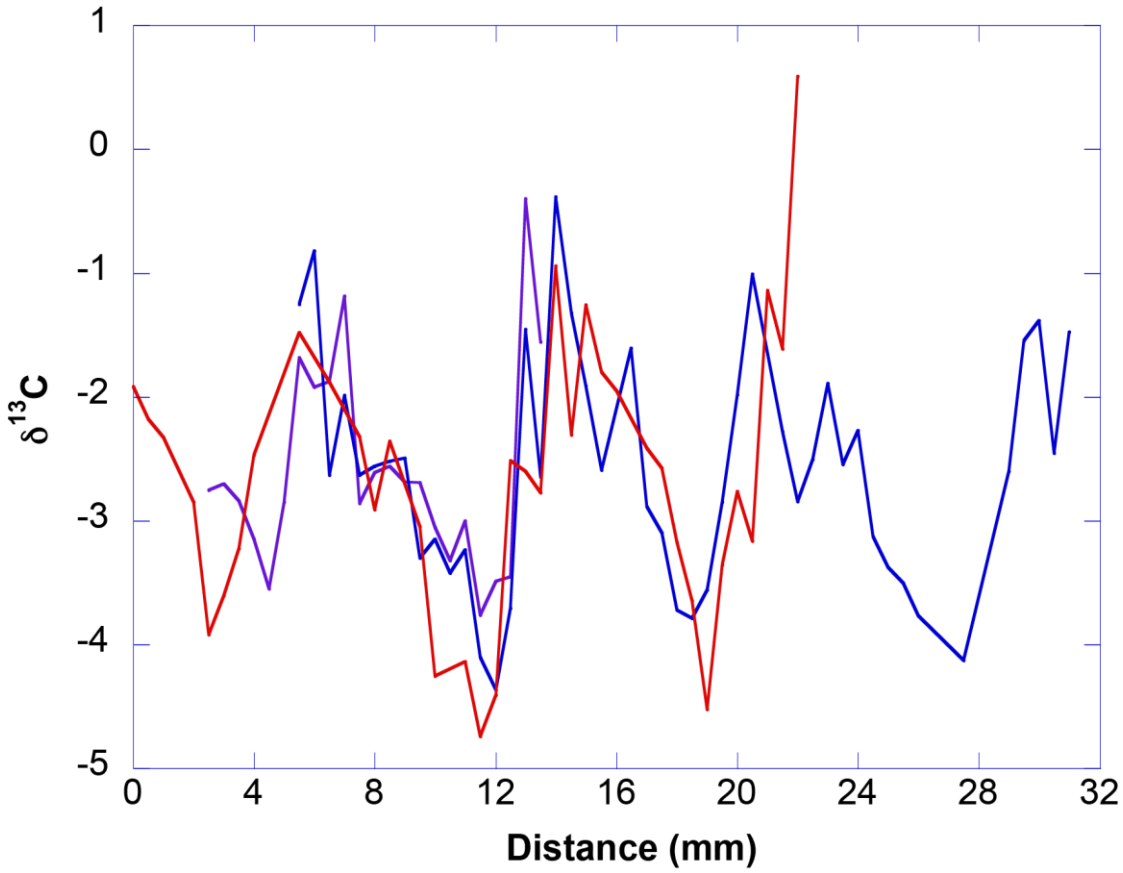

Fig. 3b. Flower Garden Banks *M. faveolata* $\delta^{13}C$ values corresponding to 1.0-mm wide x 0.5-mm long x (N)-mm deep sampling strategy sampled at (Green) 0.34-mm depth, (Blue) 0.5-mm depth, and (Red) 0.67-mm depth. There is little difference between each sampling strategy although 0.34-mm and 0.5-mm depth drill cuts show almost no difference.

sampling transect width and length down the growth axis remained constant while a different drill depth of 0.34, 0.5, and 0.67 mm were used and compared.

Results show that drill depths of 0.34 and 0.5-mm have nearly identical $\delta^{18}O$ signals while 0.67-mm depth shows more irregularity (Figure 3a-b). $\delta^{13}C$ for each of the three aforementioned transects show less variability between each drill cut depth, although, drill cut depth 0.34 and 0.5-mm are still more closely related than drill cut depth 0.67-mm. Two more transects 25-mm long were sampled side-by-side at 0.5-mm width by 0.5-mm length down the growth axis. Each transect was drilled at 0.5 and 0.67-mm depth respectively (Figures 3c,d); 0.34-mm depth was eliminated from testing at this stage after the determination that it yielded nearly identical values to 0.5-mm depth and too little coral skeletal powder for replicates and future trace metal analyses. A drill width of 0.5-mm was used for the two new transects to later compare isotope values to the previous sampled drill width of 1.0-mm. Results show that $\delta^{18}O$ of 0.5 and 0.67-mm depth samples are very close except for in summertime where 0.5-mm depth shows slightly more range than 0.67-mm depth (Figure 3d). $\delta^{13}C$ data for samples from 0.5 and 0.67-mm depth show much greater summertime variability than $\delta^{18}O$ data for samples from similar sampling depth ranges; 0.5-mm depth samples have more than 1.0‰ greater enrichment when compared to 0.67-mm depth. Comparison of the isotope range for the 0.5-mm versus 1.0-mm wide sampling transect for samples that were 0.5-mm long and 0.5-mm deep displayed only negligible differences. A drill cut dimension of 1.0-mm width by 0.5-mm depth by 0.5-mm down core distance was subsequently

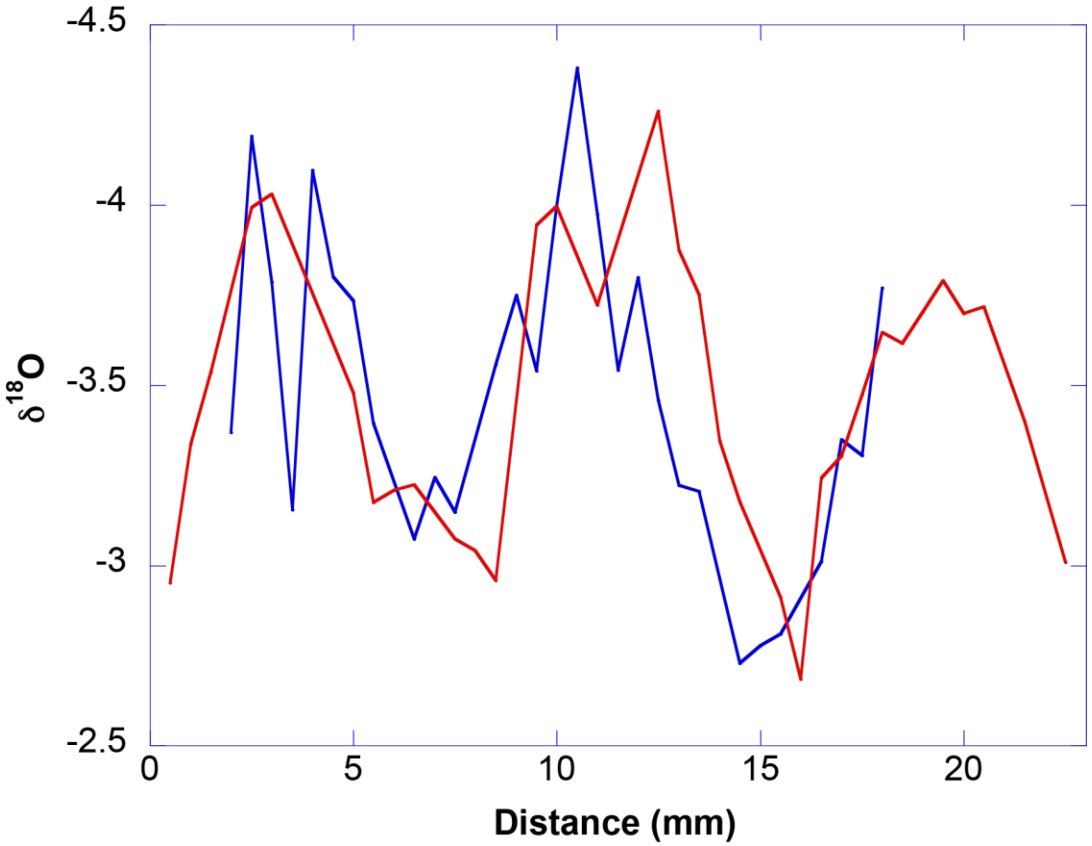

Figure 3c. Flower Garden Banks *M. faveolata* $\delta^{18}O$ 0.5-mm wide x 0.5-mm long x (N)-mm deep sampling strategy sampled at (Blue) 0.5-mm depth, and (Red) 0.67-mm depth. There is little difference between each sampling strategy for oxygen.

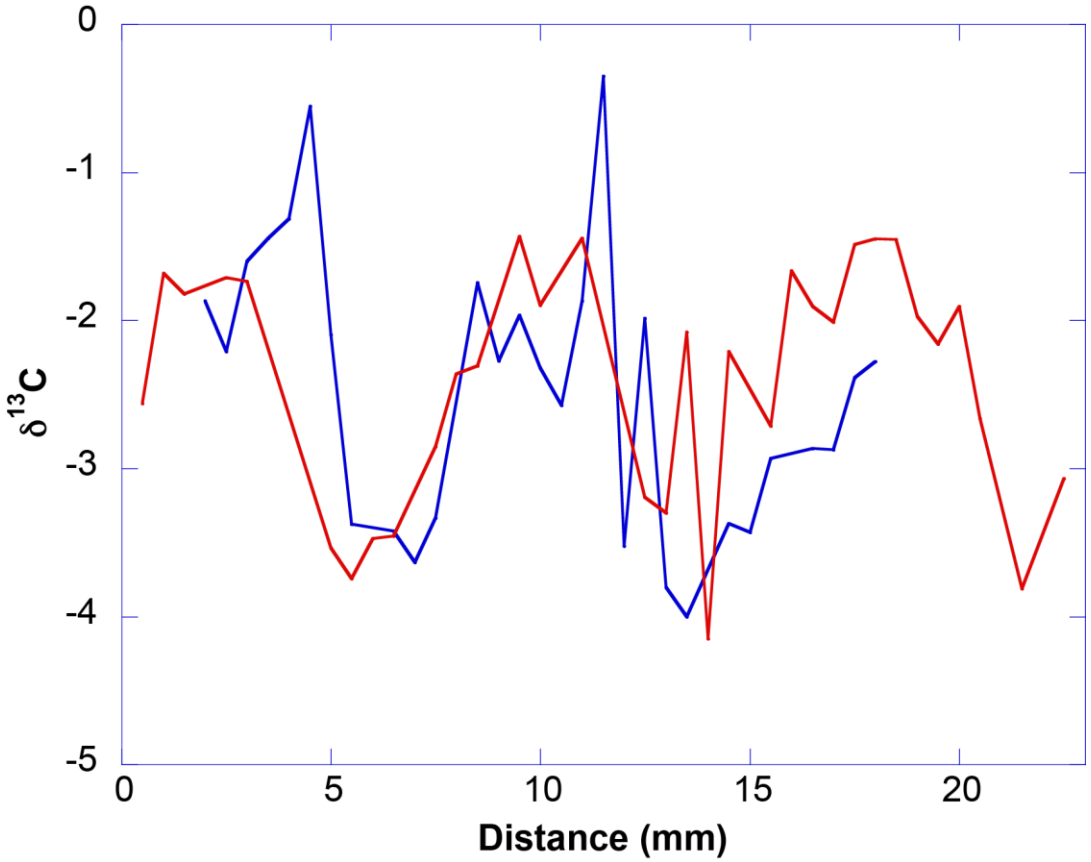

Figure 3d. Flower Garden Banks *M. faveolata* $\delta^{13}C$ 0.5-mm wide x 0.5-mm long x (N)-mm deep sampling strategy sampled at (Blue) 0.5-mm depth, and (Red) 0.67-mm depth. Carbon shows more variability than oxygen in summer months.

used for routine sampling during this study because coral skeletal samples from this drill cut dimension yielded more skeletal material (100-300 μg).

A total of 2,897 *M. faveolata* powdered skeletal samples were continuously drilled down the growth axis of the coral core for isotope analysis. Each sample yielded approximately 100-300μg of coral skeletal powder from the previously established drill cut dimensions of 1.0-mm wide by 0.5mm deep by 0.5mm long down the growth axis. An approximate chronology of the sampling path was determined by counting coral growth bands revealed by X-radiography. Each year was determined to be a couplet of high and low density bands and the beginning of each year starting from the boundary of a high density band grading into a low density band sampling from oldest coral material toward present.

Coral samples were reacted with phosphoric acid in a Kiel IV Carbonate Preparation Device to produce CO_2 gas that was then analyzed on a MAT 253 isotope ratio mass spectrometer at Texas A&M University following standard methods. To minimize the effect of mixing between reference and sample gas within the mass spectrometer source during isotope analyses [see *Ostermann and Curry, 2000*], the reference gas used for this study was created from *M. faveolata* skeletal material collected at the Flower Garden Banks so the reference and sample gases had very similar isotopic compositions. Measured ratios of ^{13}C to ^{12}C and ^{18}O to ^{16}O are presented in δ notation relative to the VPDB standard. The reproducibility of individual analyses, as indicated by the standard deviation of 584 analyses of NBS-19 standards for all sample runs, was better than 0.06‰ for $\delta^{18}O$ and 0.03‰ for $\delta^{13}C$.

3. RESULTS

The measured variations of greyscale across the *Montastrea* X-radiographic images yielded a high-resolution record of the relative variation of density across annual coral bands, which enabled growth band years and annual extension rates to be determined precisely (Table 1). For the overall record, annual growth rates averaged 8.2 mm/year (Table 1). The maximum observed growth occurred in 1897 with a one-year skeletal extension of 12.7 mm; the minimum observed growth occurred in 1960 with a one-year skeletal extension of 3.5 mm (Table 1).

The $\delta^{18}O$ of *M. faveolata* coral skeletal material from the Flower Garden Banks (Figure 4) and *in situ* seawater temperature data collected during the time period 1990-1997 from the Flower Garden Banks National Marine Sanctuary were used to calibrate an oxygen isotope-temperature equation for the region (Figure 5). Timing for the correlation of coral $\delta^{18}O$ to the *in situ* seawater temperature record was based on matching $\delta^{18}O$ extrema to annual measured temperature extrema. Finer tuning was then achieved by defining tie points to other recognizable curve characteristics in each record. All $\delta^{18}O$ sample ages between defined tie points and interpolated seawater temperatures determined from $\delta^{18}O$ sample ages were calculated by linear interpolation (implemented using Arand Interp software by *Howell et al*. [2006]).

Table 1. Flower Garden Banks *M. Faveolata* extension rate for the whole record, each decade, and pre and post 1957. Maximum and minimum growth rates are also depicted for designated time periods.

Year	Extension (mm/yr)		Average Extension (mm/yr)	Pre-1957 Extension (mm/yr)	Post-1957 Extension (mm/yr)
2005		**Average**	8.21	8.62	7.23
2004	6.795	**Maximum**	12.68	12.68	11.02
2003	7.852	**Minimum**	3.47	3.93	3.47
2002	5.738				
2001	11.023				
2000	7.399				
1999	8.607				
1998	6.04				
1997	8.607				
1996	7.399				
1995	5.889				
1994	9.06				
1993	8.758				
1992	7.097				
1991	6.493				
1990	8.003				
1989	9.211				
1988	8.003				
1987	8.607				
1986	7.097				
1985	7.55				
1984	6.644				
1983	7.55				
1982	8.607				
1981	7.399				
1980	6.644				
1979	6.342				
1978	7.701				
1977	7.399				
1976	7.55				
1975	6.644				
1974	4.681				
1973	6.493				

Table 1 Continued

Year	Extension (mm/yr)
1972	8.607
1971	5.587
1970	6.644
1969	6.191
1968	8.305
1967	8.758
1966	5.587
1965	7.852
1964	8.305
1963	8.154
1962	5.436
1961	8.909
1960	3.473
1959	4.983
1958	3.926
1957	8.154
1956	10.721
1955	9.362
1954	10.57
1953	7.55
1952	7.701
1951	8.154
1950	9.06
1949	9.362
1948	10.419
1947	6.795
1946	8.305
1945	8.154
1944	10.117
1943	9.362
1942	9.513
1941	8.456
1940	9.211
1939	10.117
1938	8.607
1937	8.758
1936	9.211
1935	8.758

Table 1 Continued

Year	Extension (mm/yr)
1934	8.154
1933	8.305
1932	9.06
1931	6.946
1930	6.795
1929	10.268
1928	7.55
1927	10.872
1926	9.211
1925	7.55
1924	8.758
1923	8.758
1922	7.55
1921	8.909
1920	9.815
1919	9.513
1918	7.701
1917	11.325
1916	11.476
1915	8.456
1914	6.493
1913	6.795
1912	7.852
1911	8.003
1910	12.684
1909	3.926
1908	7.701
1907	10.419
1906	5.436
1905	9.362
1904	11.174
1903	9.815
1902	7.55
1901	6.644
1900	10.268
1899	8.305
1898	8.003
1897	12.684

Table 1 Continued

Year	Extension (mm/yr)
1896	6.946
1895	7.248
1894	11.778
1893	8.154
1892	9.664
1891	8.607
1890	4.681
1889	6.644
1888	11.627
1887	8.909
1886	7.701
1885	4.832
1884	9.211
1883	6.946
1882	9.211
1881	6.191
1880	8.758
1879	8.456
1878	6.795
1877	7.248
1876	6.795
1875	8.154
1874	8.154
1873	8.758
1872	11.174
1871	8.456
1870	8.456
1869	7.248
1868	8.758
1867	10.419
1866	7.248
1865	6.946
1864	8.003
1863	10.268
1862	8.456
1861	8.909
1860	10.268
1859	10.117

Table 1 Continued

Year	Extension (mm/yr)
1858	7.55
1857	7.399
1856	8.758
1855	9.513
1854	8.909
1853	9.664
1852	8.909
1851	8.758
1850	8.456
1849	9.815
1848	9.06
1847	8.607
1846	6.191
1845	10.268
1844	

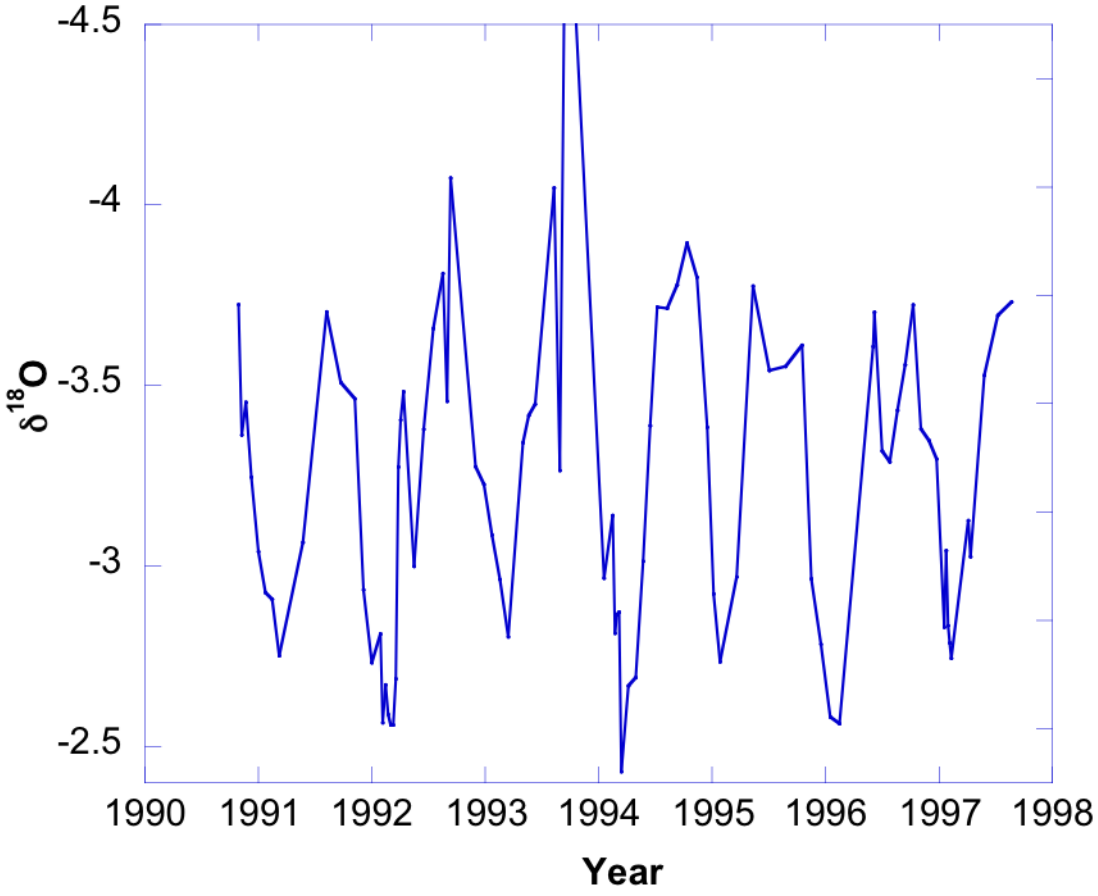

Figure 4. Coral oxygen isotope record from 1990 to 1998.

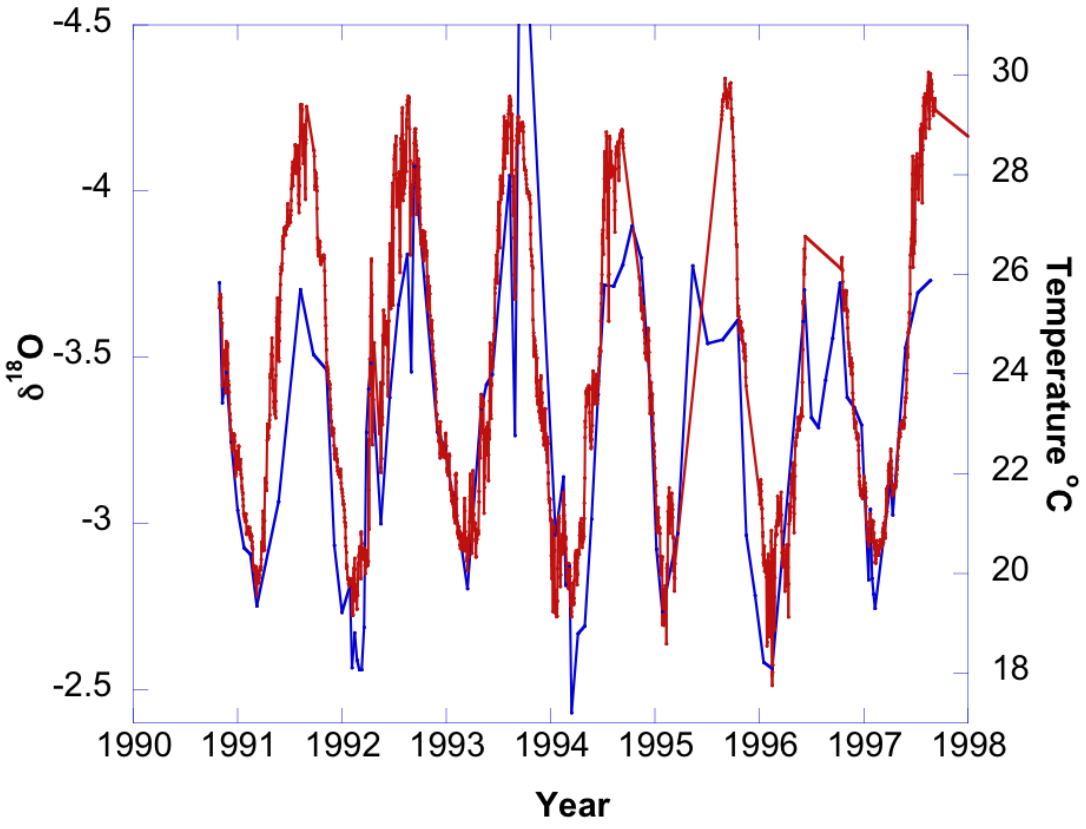

Figure 5. Comparison of *in situ* instrumental temperatures (Red) to *M. faveolata* $\delta^{18}O$ values (Blue).

The whole $\delta^{18}O$ record averages -3.24‰ and displays a range of -5.05‰ to -1.61‰ (Table 2). Summertime and wintertime $\delta^{18}O$ maxima average -3.89‰ and -2.59‰ respectively and $\delta^{18}O$ values display more variability for summertime maxima, than wintertime minima (Figure 6, Table 3). Summertime maxima have a standard deviation of 0.24 whereas wintertime minima have a standard deviation of 0.19‰. Furthermore, the maximum summertime $\delta^{18}O$ value is -3.27‰ while the minimum is -5.05‰, resulting in a range of 1.78‰. In contrast, the maximum wintertime $\delta^{18}O$ is -1.91‰ and the minimum is -3.04‰, resulting in a range of 1.13‰. Most $\delta^{18}O$ measurements fall into the range of values between -4.0 and -2.5‰ and the $\delta^{18}O$ sample measurement distribution is slightly skewed toward more positive values (Figure 7). The long term $\delta^{18}O$ record does not show a net trend (Figure 8). During the time period from 1844 to 1854, the average $\delta^{18}O$ value is -3.34‰, similarly, during the time period from 1995 to 2005, the average $\delta^{18}O$ value is -3.33‰.

The whole $\delta^{13}C$ record averages -2.26‰ and displays a range of -5.11‰ to 1.51‰ (Table 2). Annual variability of carbon isotopes from the *M. faveolata* coral studied for this paper exhibited an average $\delta^{13}C$ summertime maximum value of -0.53‰ and an average wintertime minimum value of -3.76‰ (Figure 9, Table 3). Summertime $\delta^{13}C$ maximum values display a larger interannual range than wintertime minima. The standard deviation for summertime maximum $\delta^{13}C$ values is 0.78‰ while for winter minimum values it is 0.61‰. Furthermore, the maximum and minimum values for all summertime $\delta^{13}C$ maxima are 1.51‰ and -2.61‰ respectively, resulting in a range of 4.12‰ for all summertime $\delta^{13}C$ measurements. Maximum and minimum values for

Table 2. Full record Flower Garden Banks *M. faveolata* isotope statistics**.**

	$\delta^{18}O$ (‰)	$\delta^{13}C$ (‰)
Average	-3.243	-2.263
Standard Deviation	0.447	1.077
Median	-3.262	-2.278
Maximum	-1.617	1.507
Minimum	-5.053	-5.108

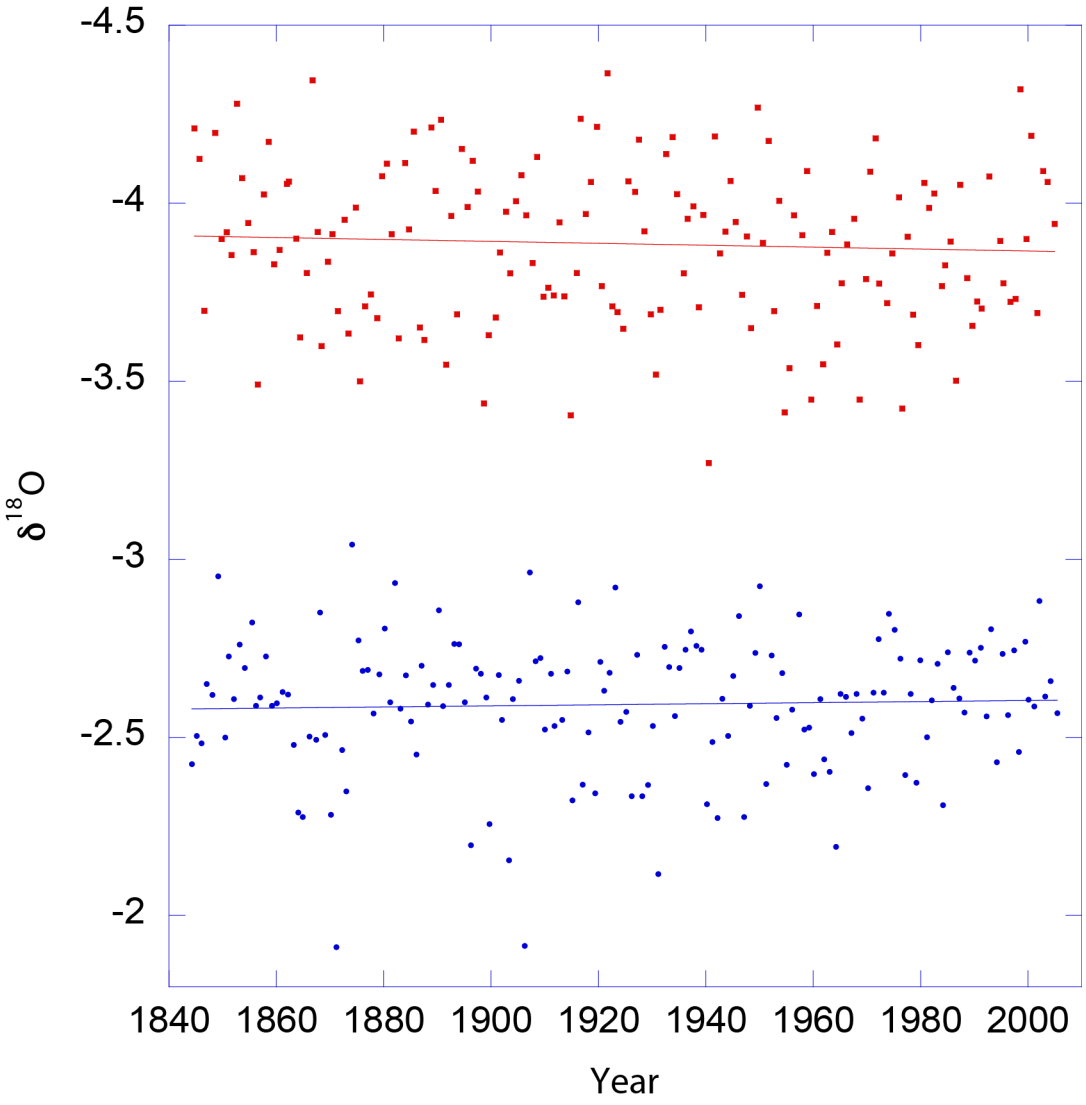

Figure 6. Annual *M. faveolata* maximum (Red) and minimum values (Blue) $\delta^{13}C$ values for Flower Garden Banks *M. faveolata* coral. Note the lack of trends for summer and winter time $\delta^{18}O$ values. Summertime trend: 0.000274x - 4.41, R = 0.053; Wintertime trend: -0.00015x – 2.30, R = 0.038.

Table 3. Flower Garden Banks *M. faveolata* summer and winter isotope extrema statistics.

	$\delta^{18}O$ (‰) Winter	$\delta^{18}O$ (‰) Summer	$\delta^{13}C$ (‰) Winter	$\delta^{13}C$ (‰) Summer
Average	-2.592	-3.886	-3.759	-0.531
Median	-2.609	-3.90	-3.676	-0.564
Standard Deviation	0.188	0.240	0.6114	0.782
Maximum	-1.911	-3.271	-2.009	1.507
Minimum	-3.0411	-5.053	-5.108	-2.609
Range	1.12966	1.783	3.100	4.115

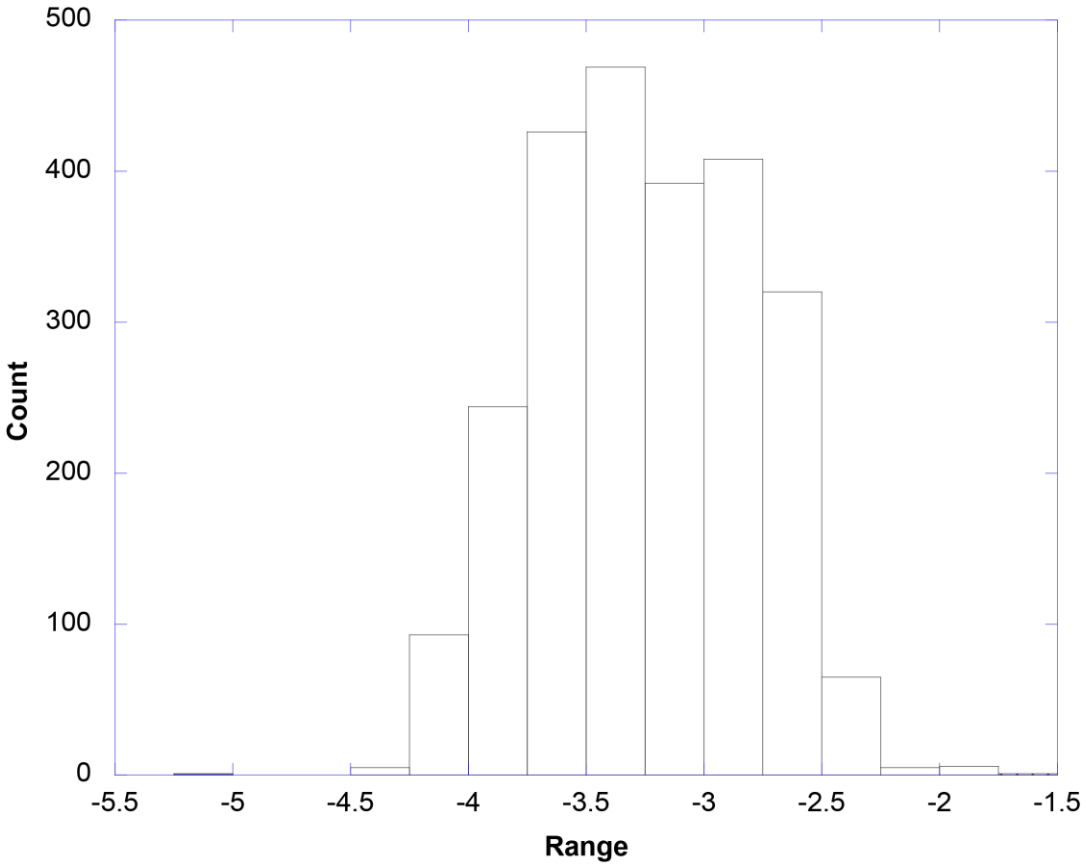

Figure 7. Distribution of the *M. faveolata* $\delta^{18}O$ values.

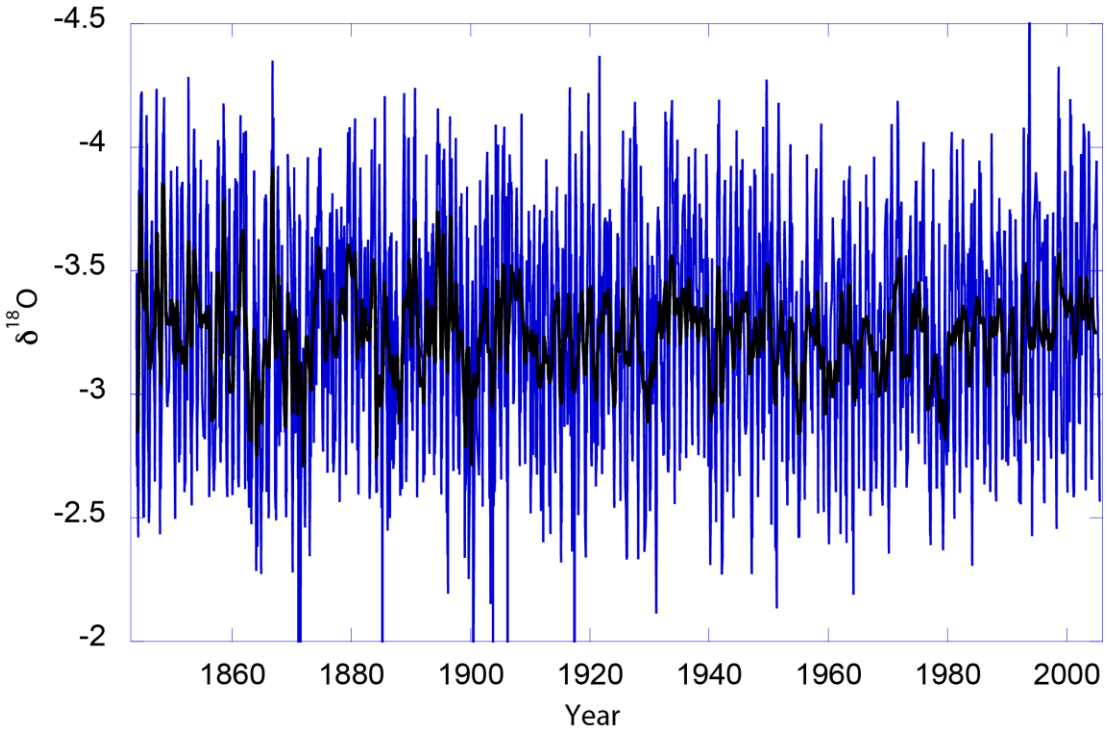

Figure 8. Time series of *M. faveolata* $\delta^{18}O$ from 1843 to 2005 (Blue). No significant long-term trend is observed with 15-point moving average applied to isotope record (Black) although interannual and interdecadal cycles are evident in the record.

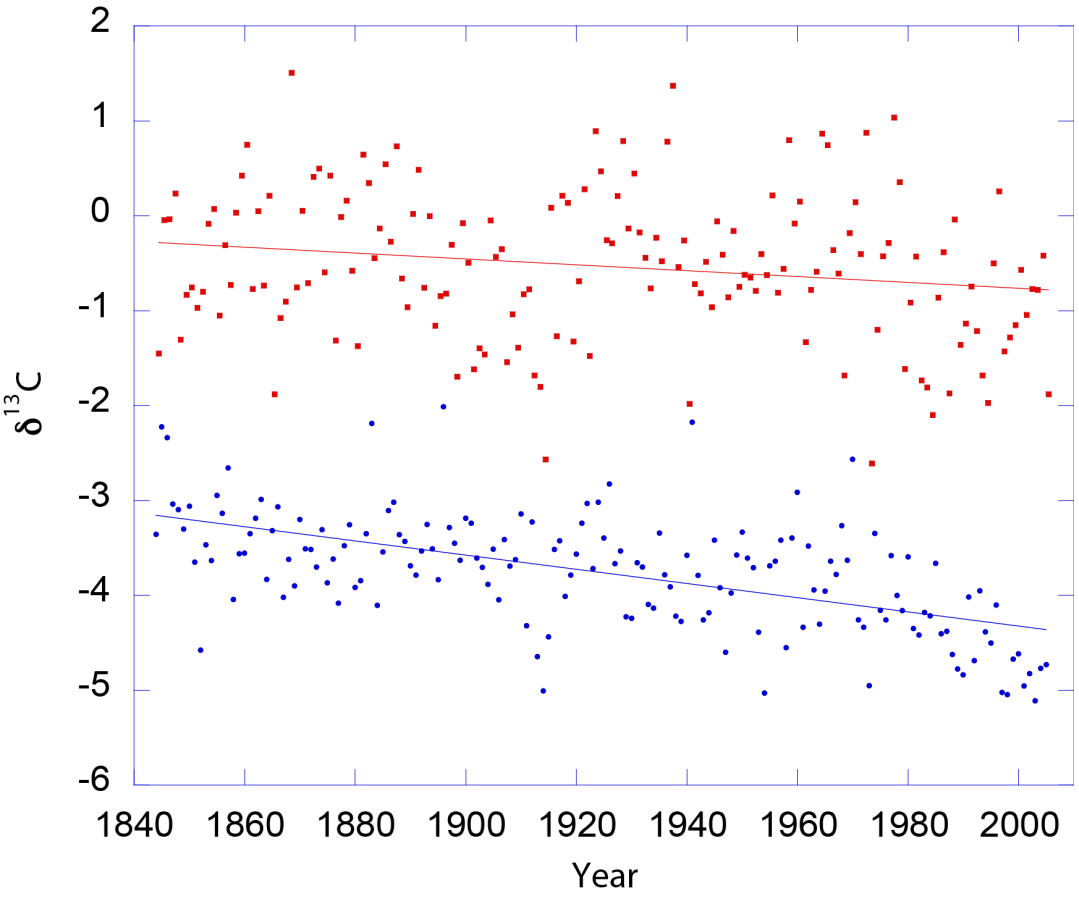

Figure 9. Annual *M. faveolata* $\delta^{13}C$ maximum and minimum values. Note the greater variability for summertime values (Red) to wintertime values (Blue). The slope of the linear fit to wintertime values is greater than twice that of the fit to summertime values. Summertime linear regression: -0.0031x + 5.41, R= 0.19; Wintertime linear regression: -0.0075x + 10.65, R = 0.57.

winter $\delta^{13}C$ are -2.01‰ and -5.11‰ respectively, resulting in a range of 3.1‰ for all wintertime $\delta^{13}C$ measurements. Most $\delta^{13}C$ measurements fall into the middle range of values between -3.0 and -1.0‰ (Figure 10). The distribution of $\delta^{13}C$ values is slightly skewed toward more positive values.

The overall $\delta^{13}C$ record shows a long term negative trend over time (Figure 11). At the earliest ten-year interval (1843 – 1853), $\delta^{13}C$ averages -1.89‰ and during the most recent portion of the record (1995 – 2005), $\delta^{13}C$ averages -3.08‰ (Table 4). There is an overall depletion of $\delta^{13}C$ values by 1.19‰ over the course of our 162 year coral record. In addition to this long-term depletion, a large negative excursion occurs between 1900 and 1920 with $\delta^{13}C$ values depleting by greater than 1.0‰ and then returning to normal values after 1920. Finally, $\delta^{13}C$ values begin to decrease more rapidly after the early 1950's.

A striking increase in the rate of $\delta^{13}C$ depletion occurs in our *M. faveolata* record during the 1902-1914 time period (Figure 11). $\delta^{13}C$ values from 1844-1902 show a slower depletion rate relative to the 1902-1914 period, as is evident in the difference of average values for $\delta^{13}C$ for the earliest ten year span, 1843-1853, which are -2.14‰ and -1.88‰, respectively. Thus, a 0.26‰ depletion of $\delta^{13}C$ occurs from the earliest decade of our record (1843-1853) to the decade leading up to the 1902-1914 depletion-event (1892-1901). The average of the $\delta^{13}C$ values for all coral material deposited before the 1902-14 depletion event (1844-1901) is -2.02‰. In contrast, the average $\delta^{13}C$ for 1902-1914 is -2.52‰, which is 0.38‰ more depleted than average $\delta^{13}C$ for 1892-1901. Interestingly, during the decade following the 1902-1914

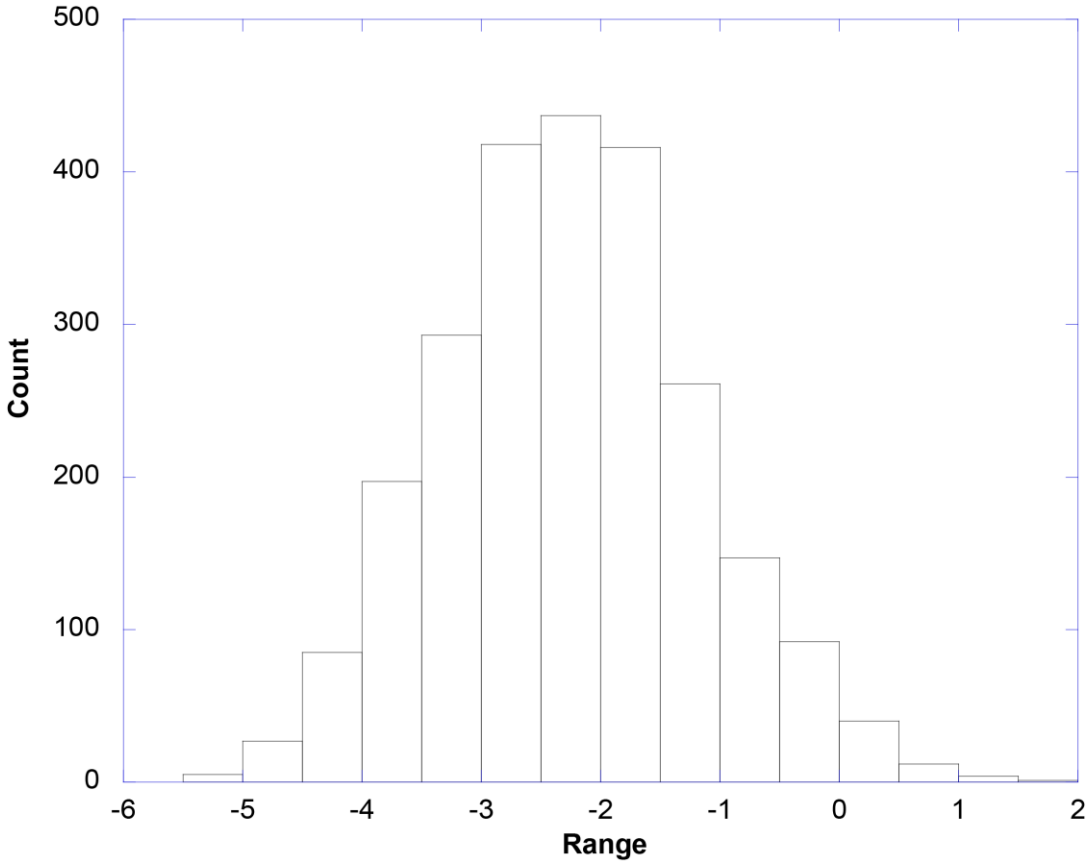

Figure 10. Distribution of *M. faveolata* $\delta^{13}C$ values.

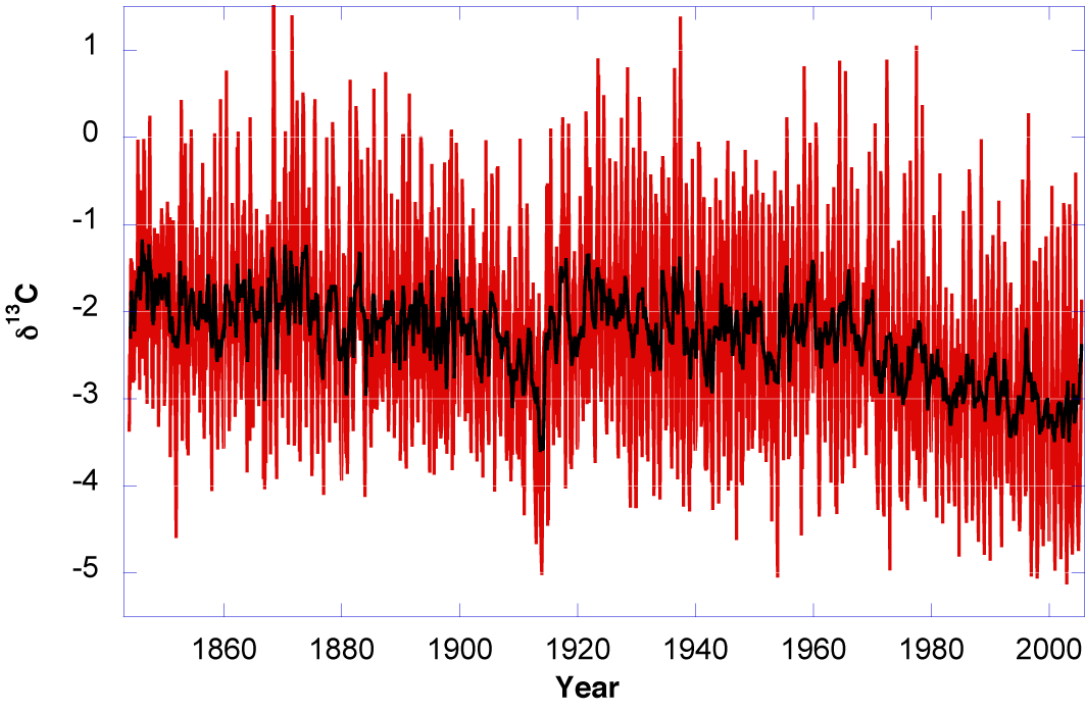

Figure 11. 15-point running average (Black) applied to time series of Flower Garden Banks *M. faveolata* coral $\delta^{13}C$ (Red) from 1843 to 2005. Long-term net depletion is evident over recorded time period.

Table 4. Summer, winter, and entire Flower Garden Banks *M. faveolata* isotope averages from earliest and most recent ten year periods in the coral record presented here. Note that most carbon isotope depletion occurs during winter.

Year	Winter $\delta^{18}O$ Average	Summer $\delta^{18}O$ Average	All $\delta^{18}O$ Average
1995-05	-2.654	-3.942	-3.331
1844-54	-2.630	-4.020	-3.337

Year	Winter $\delta^{13}C$ Average	Summer $\delta^{13}C$ Average	All $\delta^{13}C$ Average
1995-05	-4.782	-0.870	-3.08
1844-54	-3.247	-0.604	-1.866

depletion event, $\delta^{13}C$ values average -2.00‰ which is higher than decade before the depletion event.

4. DISCUSSION

4.1. Coral Sampling Strategy

Previous workers have employed many different approaches for sampling coral skeletons for chemical studies; however, they share the goals of fully resolving fluctuations of temperature and other environmental conditions [*Leder et al.,* 1996; *Quinn et al.,* 1996] and minimizing variability caused by isotopic differences in coral skeletal architecture [e.g., *Patzold*, 1992; *Leder et al*., 1996; *Cohen et al*., 2001]. It is widely accepted that sampling be conducted along the coral thecal wall to prevent isotope variability associated with the differences found between thecal wall material and endothecal material [*Patzold*, 1992; *Leder et al*., 1996]. Thecal wall sampling also helps to maintain a higher sampling resolution because the thecal wall is the densest portion of the coral cup and thus requires less sampling volume to acquire optimal mass for chemical analyses. However, coral sampling resolution remains an area that has not yet fully developed an established criterion. *Quinn et al.* (1996) suggests that a bimonthly to quarterly sampling resolution is sufficient to fully distinguish the annual $\delta^{13}C$ and $\delta^{18}O$ cycle. Conversely, *Leder et al*., (1996) maintains a sampling resolution of no less than fifty samples per year is required to fully reproduce the annual temperature extrema associated with coral $\delta^{18}O$.

The study presented here utilized a 0.5-mm drill cut intervals down the growth axis that obtained approximately 16.5 samples per year, which translates to at least monthly resolution [e.g., *Fairbanks and Dodge*, 1979; *Watanabe et al.,* 2002]. It was concluded after testing drill cut widths of 0.5 and 1.0 mm that a drill cut width of

1.0 mm was sufficient to remain within the boundaries of the thecal wall while collecting enough coral skeletal powder for isotope analyses (Figures 3 a-d). Although limiting sampling to the visible track of the thecal wall on the surface of a coral slab is easily accomplished, it is difficult to be certain of the drill depth at which thecal wall material terminates and sampling continues into other anatomical elements of the coral skeleton. Other anatomical elements of coral skeletons may contain very different isotopic values from the thecal wall which could dilute the true thecal wall isotope signal [*Patzold*, 1992; *Leder et al*., 1996]. Therefore, the study presented here tested various drill sampling depths to determine the optimal drill cut depth at which true isotope signal and appropriate sample mass for isotope analysis are both achieved. Isotope analysis of drill cut depths of 0.34, 0.5, and 0.67 mm showed that the optimal sampling dimension for the purposes of this study was 1.0-mm width by 0.5-mm length down core by 0.5-mm depth (Figures 3 a-d). The aforementioned sampling strategy assured the extraction of skeletal material from the thecal wall and regularity of isotope signal, while yielding sufficient coral powder for replicates and future trace metal analyses.

4.2. Coral $\delta^{18}O$ Temperature Equation

It is well established that $\delta^{18}O$ composition of coral skeletal material is controlled by ambient seawater chemistry and temperature at the time of accretion. *Wagner and Slowey* (2010) found that seawater at crests of the Flower Garden Banks (where the corals live) showed consistent $\delta^{18}O$ and salinity year-round with δ values averaging 1.1‰ and 36.1 PSU, respectively. Because the $\delta^{18}O$ of seawater remains essentially

constant throughout the year, relative changes in $\delta^{18}O$ of *M. faveolata* coral skeletal material at the Flower Garden Banks must be largely temperature related.

An *in situ* seawater temperature record measured from the reef crest at the Flower Garden Banks was compared to the *M. faveolata* $\delta^{18}O$ record presented here. The seawater temperature record was measured at daily resolution for the majority of the time period 1990-1997. Flower Gardens *M. faveolata* coral $\delta^{18}O$ showed good correspondence with the *in situ* seawater temperature record when finely calibrated for time (Figure 5). Linear and polynomial fit calculations of *M. faveolata* $\delta^{18}O$ and Flower Gardens *in situ* instrumentally measured temperature revealed several relationships of note. A linear fit applied to the full coral $\delta^{18}O$-seawater temperature relationship exhibited a mediocre correspondence while yielding a slope of -6.903 (Figure 12a). In contrast, a second degree polynomial curve fit calculation revealed a superior fit and confirmed that the coral oxygen isotope record presented here displays a polynomial distribution (Figure 12b).

There are several possible explanations for the observed coral $\delta^{18}O$-seawater temperature polynomial distribution presented here. Measurements of coral density down the growth axis of Flower Gardens *M. faveolata* coral skeletons reveals an average annual extension rate of approximately 8-mm per year (Table 1). Furthermore, comparison of stable isotope data to coral density confirms that *M. faveolata* exhibits an annual growth pattern of high extension rate, lower-density growth during winter and low extension rate, higher-density growth during summer (Figures 13a,b). Therefore, because summertime growth is slow in Flower Gardens *M. faveolata* corals, the coral

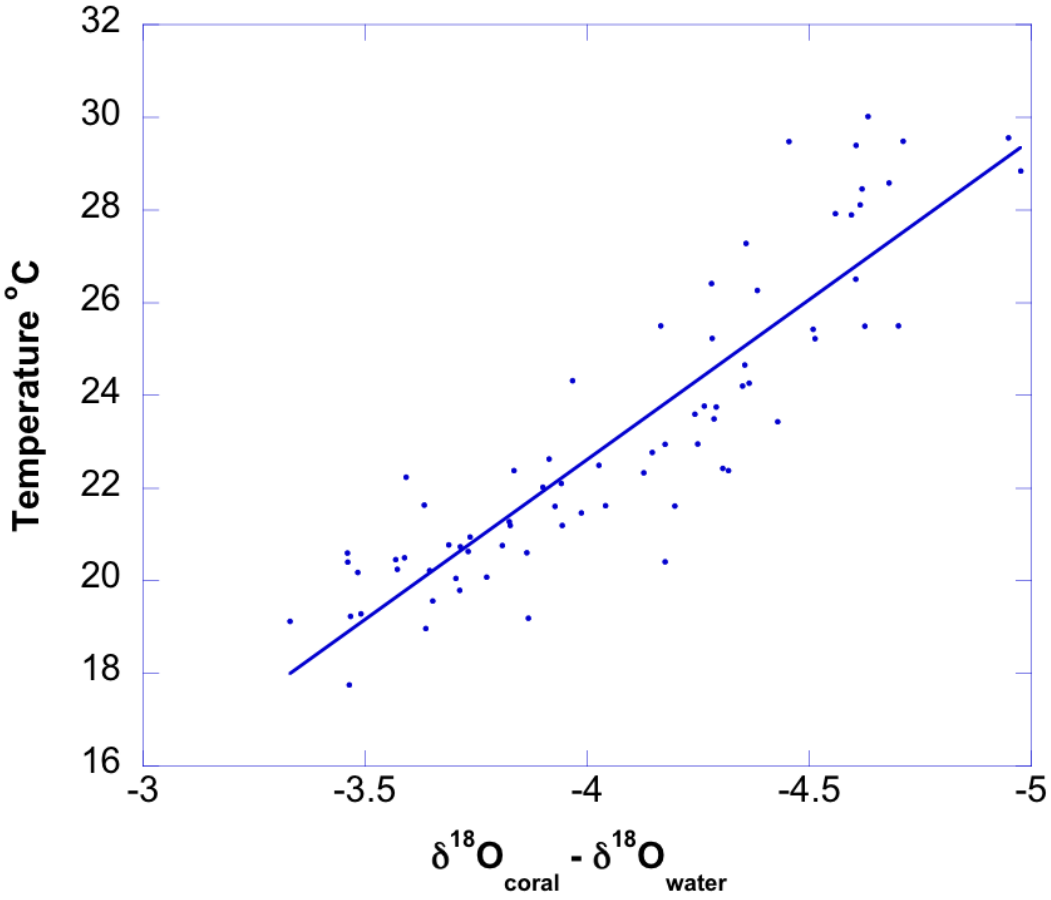

Figure 12a. Derivation of linear temperature equation for *M. faveolata* at the Flower Garden Banks. Reef crest temperature values were interpolated from existing daily temperature data to synchronize with measured $\delta^{18}O$ values using Arand Software. Y = -6.9033 X - 4.9887; R= 0.895

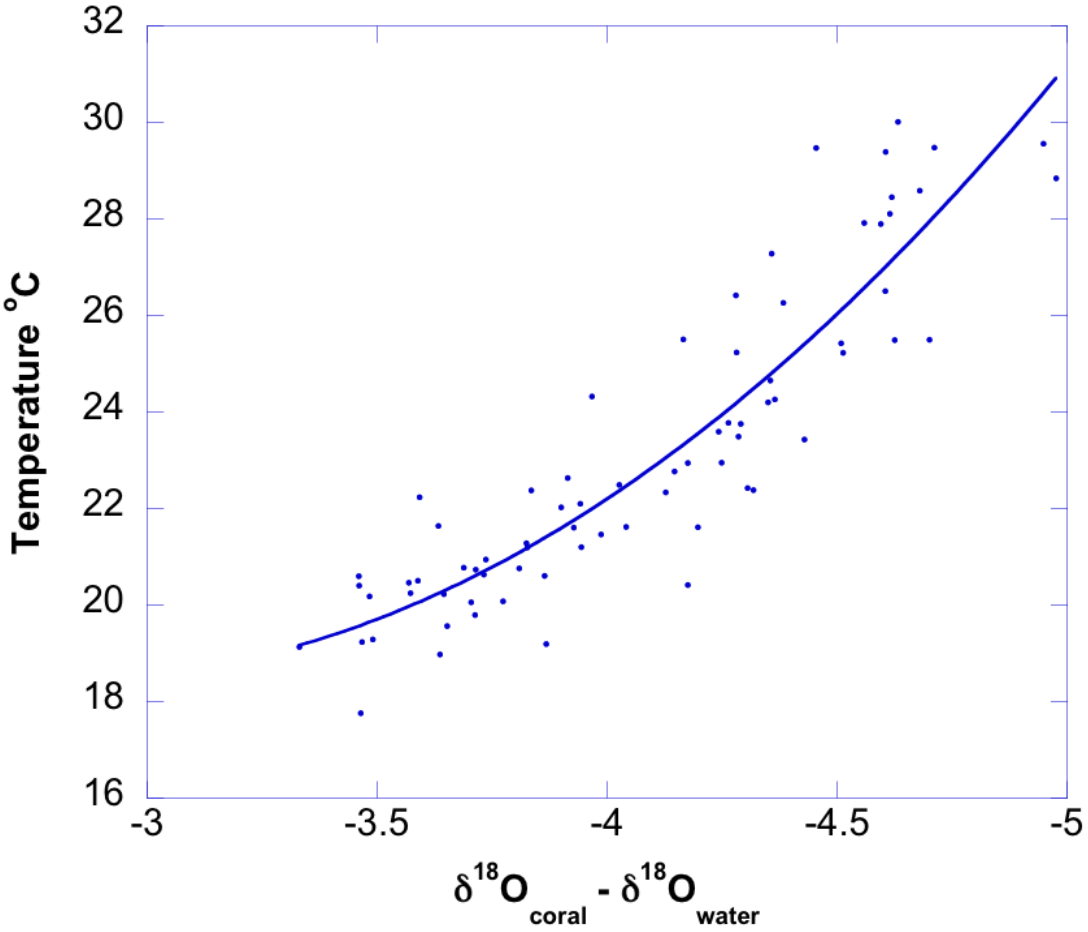

Figure 12b. Derivation of polynomial temperature equation for *M. faveolata* at the Flower Garden Banks. Second degree polynomial fit of full temperature range and corresponding oxygen isotopes for 1990-1998 yields:
$Y = 2.6814\ X^2 - 15.116\ X - 39.769$; R= 0.906.

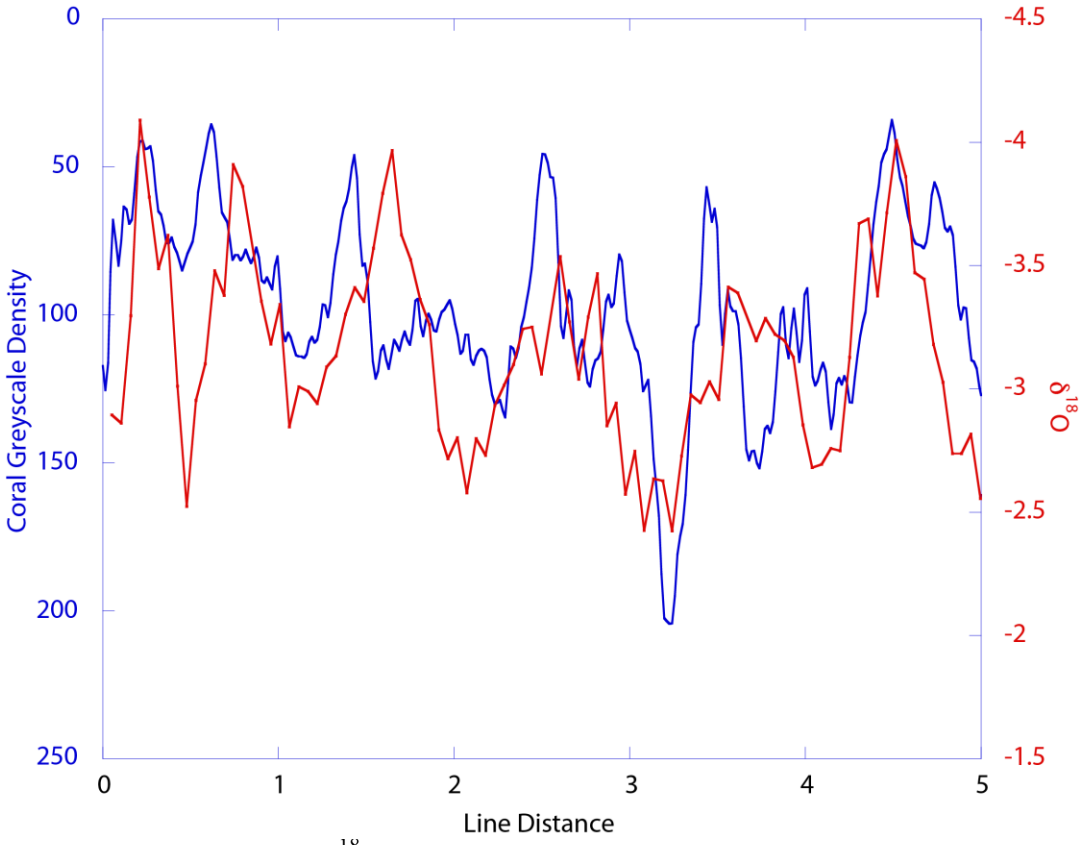

Figure 13a. Comparison of $\delta^{18}O$ (Red) and skeletal density (Blue) down studied Flower Gardens *M. faveolata* coral core in millimeter increments. Note the high synchronicity of $\delta^{18}O$ and skeletal density and the non-response of $\delta^{18}O$ to stress banding.

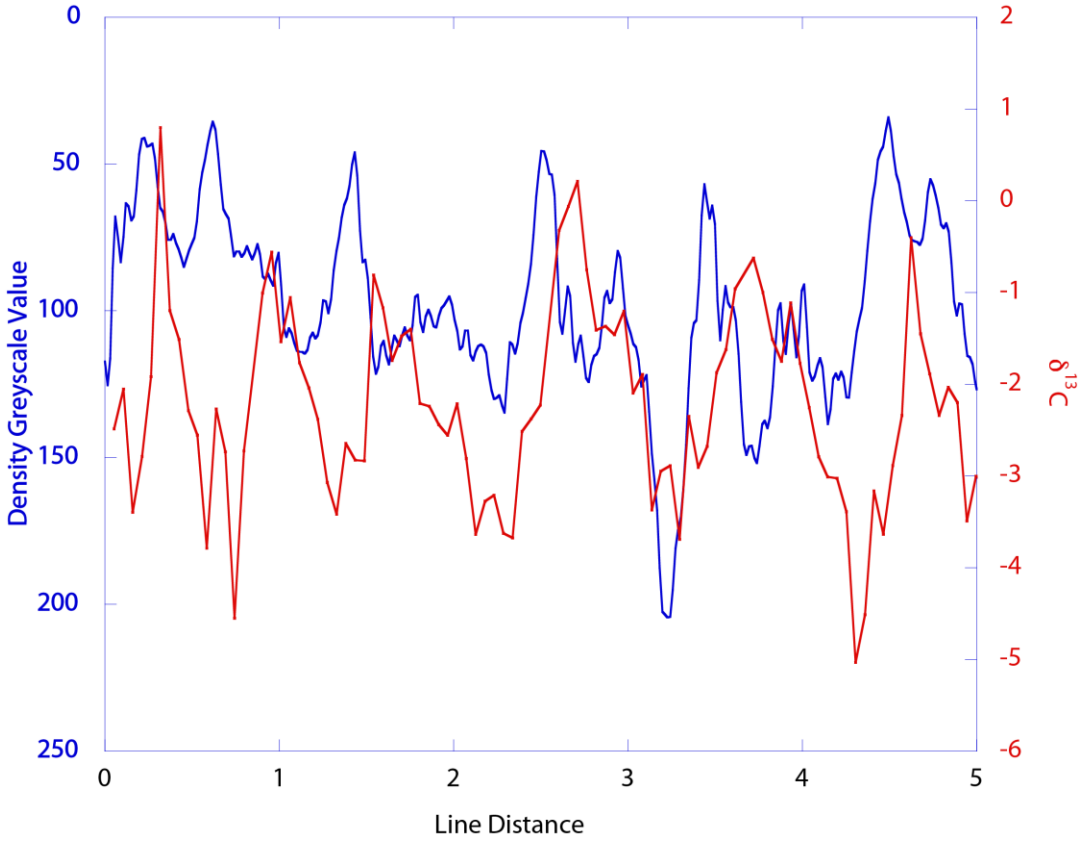

Figure 13b. Comparison of $\delta^{13}C$ (Red) and skeletal density (Blue) down the studied Flower Gardens *M. faveolata* coral core in millimeter increments. Note the lead for $\delta^{13}C$ ahead of skeletal density and the subtle response of $\delta^{13}C$ to stress banding.

oxygen isotope signal is compressed with respect to time. A consistent sampling interval on Flower Gardens *M. faveolata* corals introduces a sampling bias that results in muting of the summer isotopic signal while winter isotopes are more accurately resolved. In such a case, the oxygen isotopic relationship to temperature would exhibit an apparent high responsiveness to temperature change at low temperatures. As instrumental temperatures transitioned to summer, oxygen isotopes would show less responsiveness to temperature because the apparent summertime extrema would be dampened by isotope averaging. Another factor to consider is the kinetic isotope effect related to coral extension rate. Studies have shown that coral skeletal material is out of isotopic equilibrium with surrounding seawaters and exhibit more depleted isotope values. Disequilibrium effects have been shown to intensify with rapid growth [*McConnaughey et al.*, 1989a,b]; corals exhibiting faster extension rates display simultaneous increases in negative isotope values for $\delta^{18}O$ and $\delta^{13}C$. Therefore, Flower Gardens *M. faveolata* corals that extend more slowly in summer are likely to show more enriched isotope values than otherwise expected. In such cases, responsiveness of $\delta^{18}O$ to temperature would decrease in summer which would contribute to a polynomial distribution of oxygen isotopes to temperature. Future studies could resolve the summertime isotope-temperature effect by sampling at a much higher rate than the rate used in this study (16.5 samples per year). A higher sampling rate would eliminate sampling bias and prove or disprove a kinetic isotope effect. If a kinetic isotope effect does exist, then *M. faveolata* coral isotope records from the Flower Garden Banks would have to take this into account thus confirming the isotope polynomial distribution presented here.

4.3. Depth Versus $\delta^{13}C$

Previous work has shown that $\delta^{13}C$ values in coral skeletal carbonate vary as a function of water depth [e.g., *Land et al.,* 1975; *Weber et al.,* 1975; *Land et al.,* 1977; *Fairbanks and Dodge,* 1979]. Their findings demonstrate that with increasing depth, relative light intensity decreases, and thus, photosynthesis also decreases. Since our corals are derived from a single depth at the reef crest, it is not possible to explicitly recreate results similar to those of *Land et al.,* (1975). However, another approach could be taken to prove the existence of water depth effects on $\delta^{13}C$. Previous coral geochemical reconstructions in the Gulf of Mexico region have been primarily focused in the Caribbean Sea and Florida Straits [e.g. *Leder et al.,* 1996; *Swart et al.*, 1996; *Moyer and Grottoli*, 2011; *Giry et al*., 2013]. Coral reefs in these locations are found in shallow marine environments where the reef crest is typically no more than 3m depth below the sea surface [e.g., *Leder et al.,* 1996, *Swart et al*., 1996]. At shallow water depths, as insolation varies seasonally, the temperature of the seawater that surrounds the corals responsively changes as well. One of the unique aspects about the coral we selected for this study is the depth below sea level from which it was collected. The *M. faveolata* coral core used for this project was extracted from ~20-m depth [*Rezak et al.*, 1985]. At this depth, an assumed lead-lag insolation and temperature relationship should be apparent if surface irradiance and sea water temperatures respond to insolation at different rates. Therefore, although corals at the Flower Garden Banks should record shifts in $\delta^{13}C$ immediately it will take more time for coral skeletons at these depths to record similar shifts in $\delta^{18}O$.

If such a hypothesis is valid, then all coral records should display a relative lead-lag relationship for $\delta^{13}C$ and $\delta^{18}O$, the difference in timing of which is dependent upon depth. However, previous studies have shown widely varying results, such as synchronous seasonal changes for $\delta^{13}C$ and $\delta^{18}O$ [e.g., *Shen et al*., 1992] and $\delta^{18}O$ showing a lead time ahead of $\delta^{13}C$ [e.g., *Swart et al*., 1996]. Furthermore, personal correspondence with other workers suggest that there is a wealth of unpublished coral stable isotope data that show little coherence within the context of their surrounding environment.

We believe that a possible cause for such confusing datasets could be depth related. For example, corals that are collected in shallow regions are affected by multiple nearshore processes such as waves, tides, and terrestrial freshwater and chemical inputs, which could result in an unclear relationship between $\delta^{13}C$ and $\delta^{18}O$, much less a coherent dataset that reflects seasonal and longer-term environmental variability. In contrast, corals that are collected farther offshore are more or less unaffected by waves, tides, and terrestrial freshwater and chemical inputs. Moreover, by collecting coral material from deeper waters, the mixed layer is able to establish itself, allowing for coral records to display the elegant temporal relationship between $\delta^{13}C$ and $\delta^{18}O$ and in turn, the true insolation-seawater temperature time offset at depth.

Our record shows an approximate 2 month lead for $\delta^{13}C$ ahead of $\delta^{18}O$ (Figure 14). This would suggest that depth has a temporal effect on the oxygen isotopic composition of a coral skeleton in addition to an effect on absolute $\delta^{13}C$ values. To confirm our finding, *in situ* temperature records from the Flower Garden Banks reef

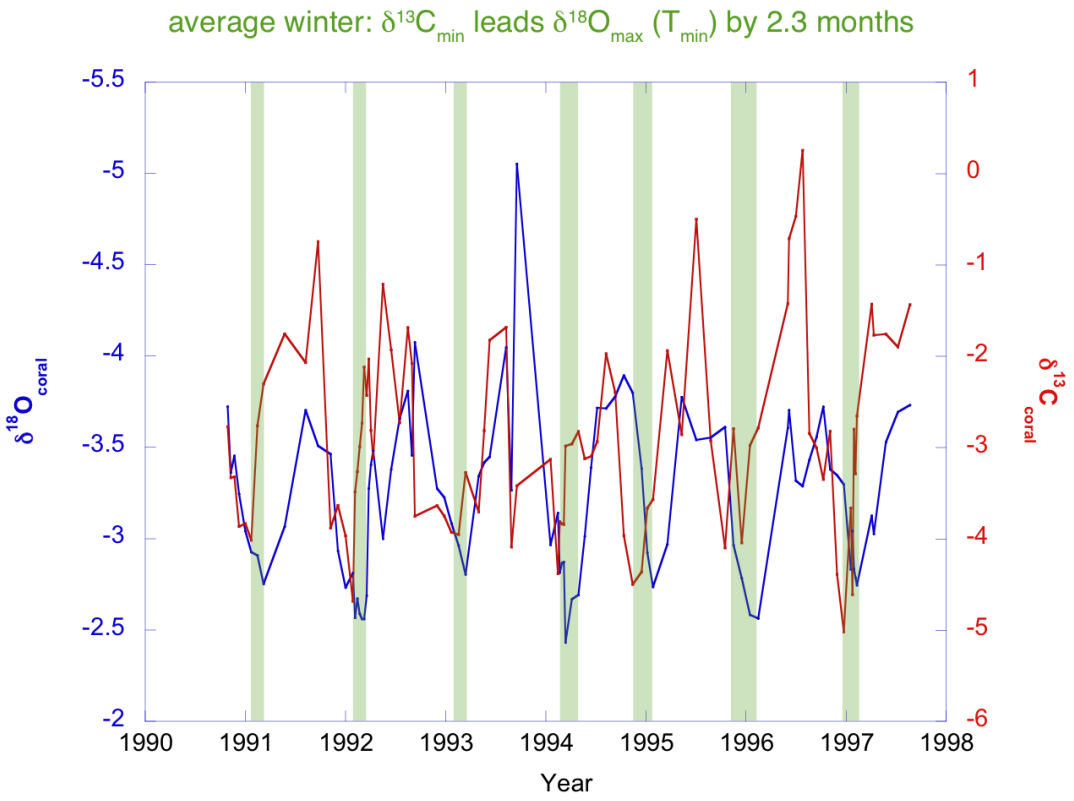

Figure 14. Time series of *M. faveolata* $\delta^{13}C$ (blue) and $\delta^{18}O$ (Red) from 1985 to 1990. Wintertime minima display a consistent offset for $\delta^{13}C$ and $\delta^{18}O$ of approximately 2.3 months (Green). Note saw tooth pattern of $\delta^{13}C$ due to abrupt depletion of $\delta^{13}C$ during the fall time period resulting in an apparent maximum lead time for $\delta^{13}C$ during the fall.

crest and an insolation model based on the latitude of the Flower Garden Banks and its relationship to variations in the position of the Earth's axis relative to the ecliptic plane were used to reconstruct a record of temperature and insolation at the reef crest (Figure 15). The model reconstruction and *M. faveolata* oxygen and carbon isotope record are in good agreement that will be discussed thoroughly in the next section.

4.4. Photosynthesis/Respiration Versus $\delta^{13}C$

There has been much debate about the controlling factors of $\delta^{13}C$ in coral skeletons and to what degree each proposed factor affects $\delta^{13}C$ composition [e.g., *Weber and Woodhead*, 1972; *Goreau,* 1977; *Erez*, 1978; *Swart*, 1996; *Grottoli and Wellington*, 1999]. Although there is general consensus that $\delta^{13}C$ is primarily modulated by photosynthesis and respiration, investigators have observed varying results with respect to the degree by which $\delta^{13}C$ is affect by photosynthesis and respiration [e.g., *Goreau,* 1977; *Swart*, 1996]. Our record provides unique insight into this matter because $\delta^{13}C$ is decoupled from $\delta^{18}O$ with respect to time by approximately 2 months (Figure 14, Table 5). If we are able to calibrate oxygen isotopes well with *in situ* seawater temperature records, then carbon isotopes should also be well calibrated to independent photosynthesis measurements/models if photosynthesis is the dominant environmental factor controlling carbon isotope fractionation. Furthermore, if a linkage between P/R and $\delta^{13}C$ is found, then a strong case for $\delta^{13}C$ as a time marker can be made.

The instrumental record from the Flower Garden Banks National Marine Sanctuary available from the reef crest at the

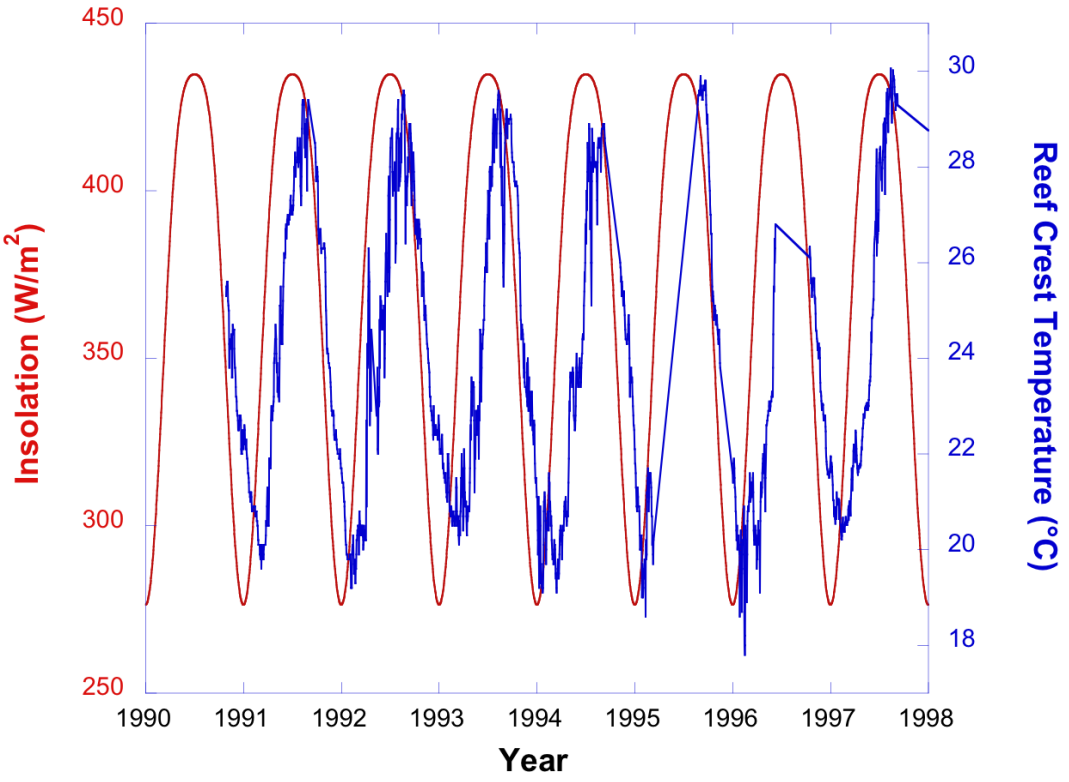

Figure 15. Time series of Flower Garden Banks instrumentally measured reef crest water temperature (Blue) and modeled solar insolation (Red). Insolation leads instrumentally derived temperature by approximately two months.

Table 5. Isotopic timing of $\delta^{13}C$-solstice calibration and $\delta^{13}C$-summer spawning calibration.

Normal Calibration	**Carbon in Years**	**Carbon in Months**	**Oxygen in Years**	**Oxygen in months**
Average Summer Maxima Date	0.47	~June 21st	0.639	~August 21st
Average Winter Minima Date	0.97	~December 21st	0.168	~February 1st

Spawn Calibration	**Carbon in Years**	**Carbon in Months**	**Oxygen in Years**	**Oxygen in months**
Average Summer Maxima Date	0.64	~August 21st	0.809	~October 22nd
Average Winter Minima Date	Not Applicable	Not Applicable	0.328	~April 28th

West Flower Gardens Banks was compared with the *M. faveolata* carbon and oxygen isotope data (Figure 15). Instrumental temperature values show a consistent annual cycle with an average low and high value of approximately 19.2^{o}C and 29.5^{o}C respectively. Because measured insolation data from the reef crest is unavailable, an insolation model was created based on the position of the Earth's axis relative to the ecliptic plane [e.g., *Berger*, 1979]. Assuming a solar constant of 1370 W/m^2, at 27.9^{o} latitude, and a phase shift of half a year (182.625 days), zenith angle was calculated with the following equation:

Zenith Angle = (Latitude^{o}-23.5^{o})*cos(2π*((day of year)-(182.625 days))/(365.25 days)

Daily insolation was then calculated as follows:

Daily Insolation = (1370 W/m^2/π)*(cos(2π*(zenith angle))/365.25 days)

The calculated insolation values displayed an annual cycle with values varying between 276 and 435 W/m^2 annually (Figure 16).

Minimums in our Flower Garden Banks insolation model occur at the winter solstice. This is approximately 11.6 months after the start of the year, or equivalently December 21st of every year (Figure 16; Table 5). Temperature minimums occur on average 1.77 months after the beginning of any respective year (Figure 15; Table 5). This result demonstrates an approximate 2.1-month lead-time for insolation ahead of

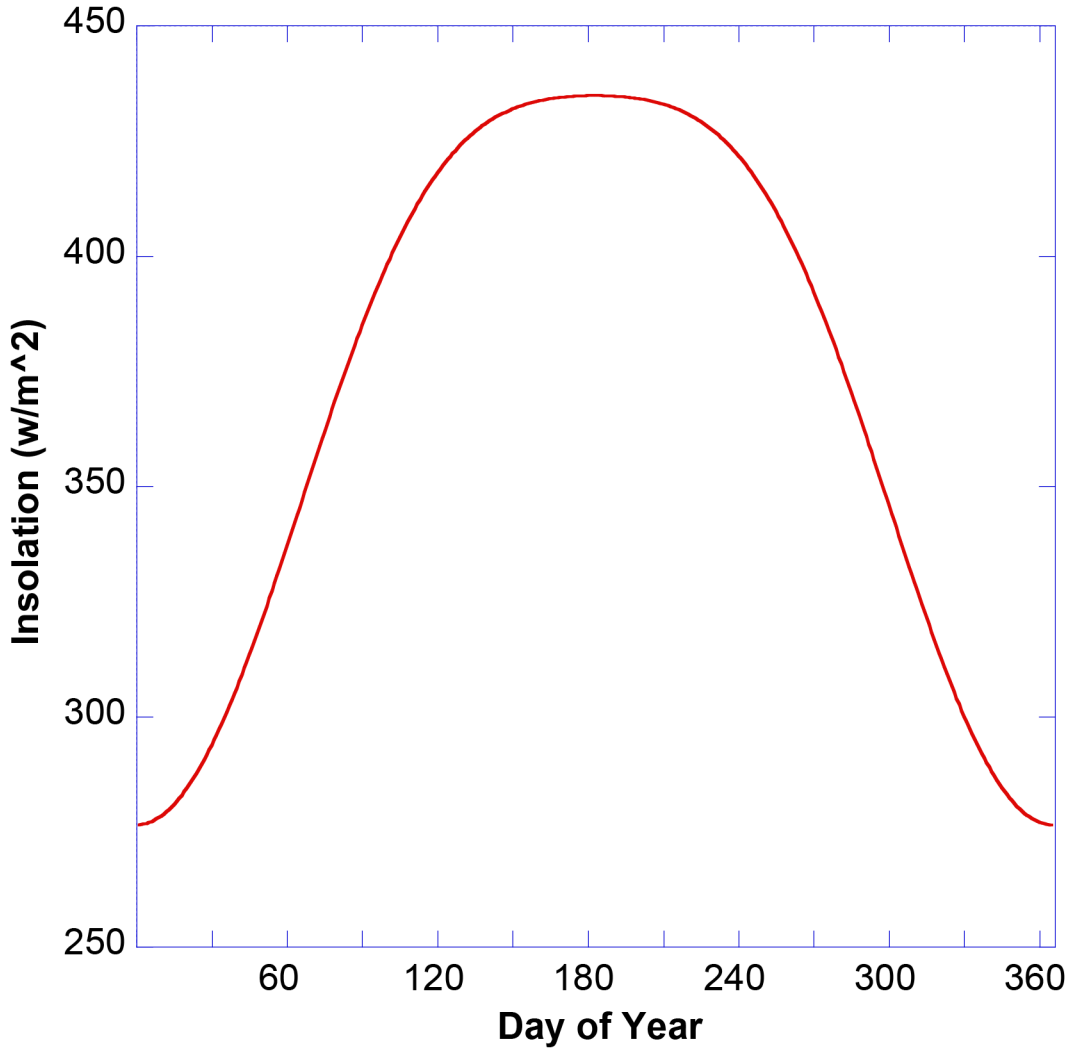

Figure 16. One-year modeled isolation variation at the Flower Garden Banks as calculated by the methods of *Berger*, [1979].

water temperature during winter months. Similarly, insolation maximums in our Flower Gardens Banks model occur during the summer solstice (Figure 16, Table 5). This value is approximately 5.6 months after the beginning of each year, or equivalently June 21st of every year. Temperature maximums occur, on average, 7.6 months after the beginning of the year (Figure 15, Table 5). This result shows an identical 2.1-month lead time for changes in insolation ahead of changes in water temperature for both summer and wintertime. Thus, after a change in insolation occurs, it takes approximately 2 months time for seawater at the depth of the reef crest to show a similar temperature change. This delay is the amount of time needed for ambient seawater at the reef crest of the Flower Gardens Banks to accumulate enough energy to show seasonal shifts in water temperature due to the high heat capacity of the water.

If corals at the Flower Gardens Banks are primarily tracking changes of photosynthesis/respiration ($\delta^{13}C$) as well as changes of temperature in the ambient seawater ($\delta^{18}O$) in the isotope content of their skeletons [e.g., *Weber and Woodhead*, 1972; *Dunbar et al*., 1981; *Weil et al*., 1981], then $\delta^{13}C$ and $\delta^{18}O$ should show a very similar relationship to the one shown by our insolation model and *in situ* temperature record. A new approach was used for producing an age model for pre-instrumental isotope records from corals from the Flower Gardens Banks. Using the assumption that $\delta^{13}C$ is primarily controlled by insolation, we defined each $\delta^{13}C$ maxima and minima as summer and winter solstices respectively. Results show that the number of years derived by the carbon age model technique utilized in this study corresponds well to the number of years derived from counting annual growth bands. Furthermore, comparison of $\delta^{18}O$

values that were age calibrated using the carbon isotope technique presented here with *in situ* seawater temperature measurements shows very good correlation. $\delta^{18}O$ minimums occur on average two months after the beginning of each new year and maximums occur approximately 7.6 months after each new year (Figure 4; Table 5). The timing of the $\delta^{18}O$ maxima and minima are virtually identical to long term *in situ* instrumental temperature measurements. Temperature measurements show minimum values on average occurring 1.77 months after each new year and maximum values occurring 7.6 months after each new year. Knowing that the timing of the $\delta^{18}O$ record is nearly identical to the timing of the *in situ* temperature record when a $\delta^{13}C$-annual insolation age model is used further corroborates that $\delta^{13}C$ variability is primarily controlled by annual insolation and can be used as a highly precise age calibrating method.

A comparison of Flower Gardens coral annual $\delta^{13}C$ cycles to modeled insolation values show very good correlation overall (Figure 17), however, there are inconsistencies between the records that are not explained by a $\delta^{13}C$-insolation linkage. Comparison of minima and maxima data points within the $\delta^{13}C$ and insolation datasets and the $\delta^{18}O$ and SST datasets show strong temporal correlation (Figures 5&17), as do the $\delta^{13}C$ -$\delta^{18}O$ (Figure 14) and SST-Insolation (Figure 15) temporal offsets. However, the transitional periods between maxima and minima present a different relationship for $\delta^{13}C$ -$\delta^{18}O$ than SST-Insolation. During the transitional fall time-period, $\delta^{13}C$ displays an abrupt shift to more negative values while $\delta^{18}O$ exhibits more gradual decline (Figure 14). As a result, $\delta^{13}C$ and $\delta^{18}O$ signals appear to have a larger temporal offset for fall than for spring. Instrumental temperature and modeled insolation show no such

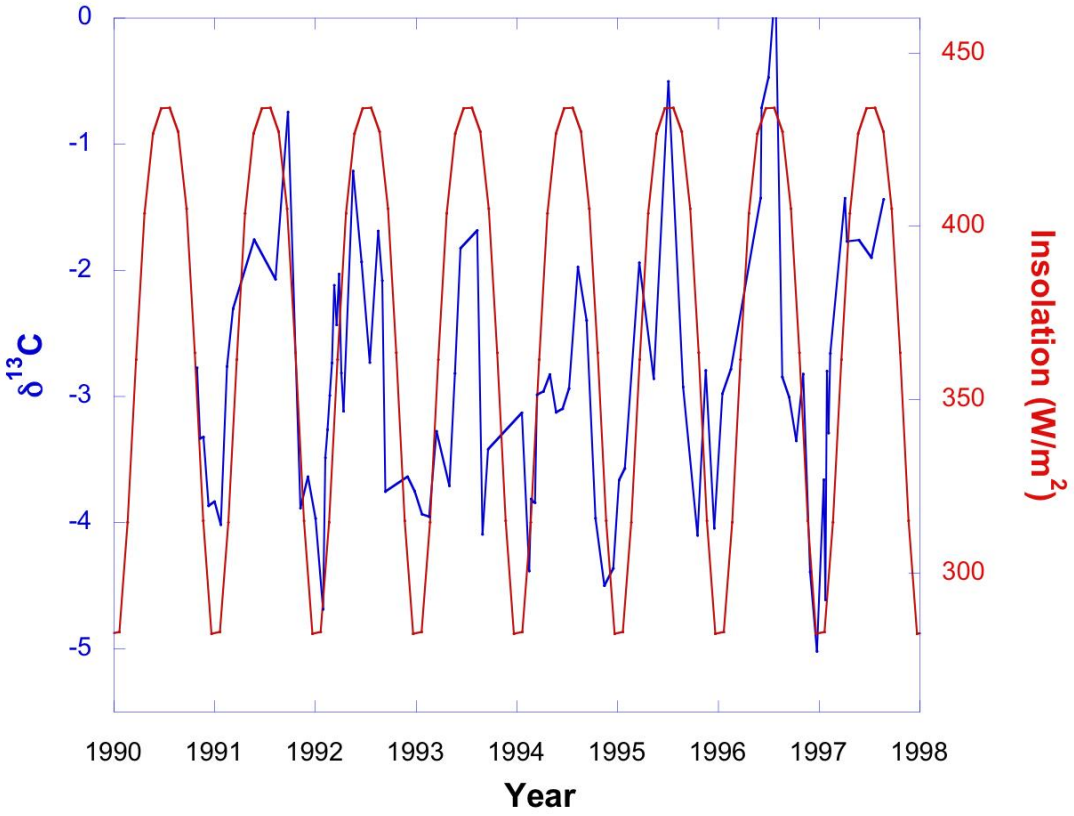

Figure 17. Time series of *M. faveolata* $\delta^{13}C$ (Blue) and Flower Garden Banks insolation (Red) from 1990 to 1998. For most of each annual cycle, $\delta^{13}C$ acts as a faithful proxy for insolation until fall time where an abrupt depletion is present.

asymmetry in their recorded annual cycle. A consistent 2-month phase shift exists between the instrumental temperature and modeled insolation records (Figure 15). A comparison of the $\delta^{18}O$ and instrumental temperature records show a high level of correlation during an annual cycle (Figure 5). Conversely, a comparison of $\delta^{13}C$ versus modeled insolation reveals distinctive annual cycles that are synchronous and show good correlation until the transition from summer to winter occurs (Figure 17). Insolation values show smooth and symmetrical annual variation. $\delta^{13}C$ of coral skeletal material from the Flower Garden Banks display abrupt change to negative values for each annual transition from summer to winter. This suggests that other variable(s) are affecting $\delta^{13}C$ during the fall. Such possible variables could include increased fall time cloudiness, changes in feeding habits, changing ambient DIC conditions, residual isotope effects caused by the early August spawn, and increased extension rate disequilibria effects [e.g., *Goreau*, 1977; *Fairbanks and Dodge*, 1979; *McConnaughey*, 1989a,b; *Gagan et al*., 1996; *Grottoli and Wellington*, 1999].

Comparison of $\delta^{18}O$ cycles to *in situ* instrumental temperature records provides an independent reference for timing of isotope records. When $\delta^{18}O$ records are tuned to *in situ* temperature records, we find that $\delta^{13}C$ peaks and valleys are well-synchronized with summer and winter solstice dates, which correspond to the times of maximum and minimum insolation levels. A positive relationship exists between $\delta^{13}C$ and insolation (Figure 17) that is consistent with coral carbon isotope fractionation models proposed by *Weber and Woodhead* (1970) and later modified by *Goreau* (1977a,b). Each author contends that insolation levels modulate photosynthesis, which in turn determines coral

skeletal $\delta^{13}C$. The findings here contrast with the findings of *Erez* (1978) who suggests that greater photosynthesis would increase the amount of metabolic CO_2 in the coral's internal carbon pool, resulting in lower $\delta^{13}C$ during high insolation periods.

4.5. $\delta^{13}C$ as a Time Indicator

To determine age increments in coral skeletons, studies typically rely on counting annual coral growth bands or take $\delta^{18}O$ or Sr/Ca fluctuations to be seasonal temperature cycles [e.g., *Tudhope et al.,* 1995; *Swart et al.,* 1996; *Crowley et al.,* 1997; *Stephans et al.,* 2004]. A very few studies take $\delta^{13}C$ fluctuations to be indicators of annual periods of time [*Cole et al*., 1993], but in general, ambivalence exists toward $\delta^{13}C$ as a time indicator. A comparison of the Flower Gardens *M. faveolata* coral results presented here with coral isotope records from the equatorial pacific reveals that as the latitude of a site and the magnitude of seasonal insolation fluctuations increase, the $\delta^{13}C$-insolation relationship provides a seasonally-resolved indicator of coral age (Figure 17; Table 5). The time indications provided by $\delta^{13}C$ can be particularly valuable in situations where corals exhibit complicated patterns of skeletal density or $\delta^{18}O$ variability, such as when winter stress banding or events of freshwater influx occur. It should be noted that during periods of freshwater flux $\delta^{13}C$ can also be affected, however, because insolation and $\delta^{13}C$ should show a high correspondence in ideal environments, an offset of $\delta^{13}C$ from insolation patterns can also be useful as an indicator of past freshwater fluxes to a study region. Also, because the extremes of $\delta^{13}C$ lead those of $\delta^{18}O$ by 2 months, the combination of $\delta^{13}C$ and $\delta^{18}O$ age indicators allows for sub-annual age discrimination.

4.6. Coral Spawning Relative to Annual Maxima of $\delta^{13}C$

It has been suggested that maxima of annual $\delta^{13}C$ cycles denote time periods of coral spawning [*Gagan et al*., 1996]. The reproductive tissues of a coral are partially composed of lipid droplets [*Szmant*, 1986] and these lipids are enriched in ^{12}C [*Swart*, 1983]. *Gagan et al*. (1996) showed a close correspondence between maximum $\delta^{13}C$ values and spawning periods of *Porites* corals from the Great Barrier Reef and Indian Ocean, and proposed that this occurred because incorporation of ^{12}C into lipids leaves the $\delta^{13}C$ of the remaining calcifying pool isotopically heavy.

Does this proposed mechanism operate at the Flower Garden Banks? Coral broadcast spawning at the Flower Garden Banks occurs 7-10 days after the August full moon [*Gittings,* 1992; *Vize et al*., 2005]. If the spawning period corresponds with annual $\delta^{13}C$ maxima, then each Flower Garden coral $\delta^{13}C$ maximum should correspond to this time period. Because the age model that we produced is based on calibrating the annual maximum of coral $\delta^{13}C$ to the time of maximum insolation, by definition the $\delta^{13}C$ maxima will not match up with the spawn date for *M. faveolata* at the Flower Garden Banks. Therefore, an independent means of establishing when spawning occurs relative to the $\delta^{13}C$ maximum is required. *In situ* temperature measurements at the Flower Garden Banks reef crest reveal seawater temperature maxima to occur in mid-August and minima to occur in early March (Figure 15). Presuming seawater temperature is the primary control on coral $\delta^{18}O$ then the annual minima in $\delta^{18}O$ also occur in August, as does coral spawning. Because the results of this study indicate that these events precede

the coral $\delta^{13}C$ maxima by more than 2 months, coral spawning does not appear be a primary control on the $\delta^{13}C$ of *M. faveolata* coral at the Flower Garden Banks (Table 5).

4.7. Coral Extension and $\delta^{13}C$

Variations in coral density banding and annual extension rates have been interpreted as physiological responses to seasonal changes of environmental conditions including: sexual reproduction and seasonal changes in photosynthesis and seawater temperature [e.g., *Knutson and Smith,* 1972; *Buddemeier and Kinzie*, 1976; *Hudson et al.,* 1976; *Hudson and Robbin*, 1980; *Dodge and Lang*, 1983; *Glynn and Wellington,* 1983; *Barnes and Lough*, 1993]. Corals from different parts of the world can exhibit completely different seasonal relationships to extension compared to the assumed seasonal relationship of corals in the Gulf of Mexico [e.g., *Erez*, 1978]. Because it is not completely clear how coral extension and density variations relate to seasonality, and because no criterion has been established in the Gulf of Mexico, a comparison of Flower Gardens coral density and extension variations to the well-established seasonal variations of $\delta^{13}C$ and $\delta^{18}O$ can provide insight about when high and low density bands occur during a year. Furthermore, the intimate linkage between isotope variations and the rate of coral skeletal accretion [*McConnaughey*, 1989a,b] can also provide valuable information about the effects coral growth changes have on the annual isotope cycle in *M. faveolata*.

Coral skeletal density measurements taken along the growth axis reveal annual variations in coral skeletal density (Figure 2). Higher density bands in Flower Gardens *M. faveolata* on average represent a much smaller portion of annual growth than

adjacent lower density bands. Low-density bands, which comprise the majority of the coral skeleton display relatively consistent density during their period of growth, however, in certain years short-lived, high-density stress bands can appear within them (Figures 13a,b).

A comparison of coral density variations to accompanying stable isotope measurements taken from within each density band reveals the linkage of density banding in Flower Gardens *M. faveolata* to seasonality (Figures 13a,b). Every coral skeletal band couplet of high and low density exhibits a positive correlation with $\delta^{13}C$ and $\delta^{18}O$. High density bands match well with summertime coral stable isotopes and low density bands correspond with wintertime coral stable isotope values, although it should be noted that skeletal density shows a slight phase shift, lagging behind both $\delta^{18}O$ and $\delta^{13}C$.

It would be assumed that if coral density and extension patterns favored either seawater temperature or light intensity as a primary controlling factor, then density banding patterns would correspond well with either $\delta^{18}O$ (seawater temperature) or $\delta^{13}C$ (light intensity) changes in the coral isotope record. However, existing coral isotope records from shallow water environments do not adequately display a relative temporal offset between $\delta^{18}O$ and $\delta^{13}C$ which confounds direct isotopic interpretation of the controlling environmental variables on coral extension since differentiation of timing between carbon and oxygen isotope records is impossible in such records. Due to the depth at which *M. faveolata* corals are found at the Flower Garden Banks, the isotope record presented here provides such an offset (Figure 14), which is necessary for

understanding the underlying patterns of coral extension and the environmental factors that control it.

Although $\delta^{13}C$ and $\delta^{18}O$ variations of Flower Gardens *M. faveolata* are in good correlation with changes of density banding (Figures 13a,b), it can be inferred that Flower Gardens coral skeletal density are likely responding to the same environmental changes that affect oxygen isotopes in the region since skeletal density more closely matches $\delta^{18}O$ (Figure 13a). The high correspondence between coral skeletal density and $\delta^{18}O$ as well as the lag period between $\delta^{13}C$ and skeletal density (Figure 13b) implies that coral calcification rates are not strongly modulated by photosynthesis. Rather, it is more likely that annual seasonal seawater temperature is impacting seasonal variations of coral extension rates.

Since summertime temperatures and insolation last much longer than wintertime temperatures and insolation, and because high density/summertime bands grow much slower than low density/wintertime coral growth bands, the stable isotopic information derived from *M. faveolata* in this study exhibit a wide sampling resolution. Comparison of $\delta^{18}O$ derived temperatures to *in situ* instrumental temperatures show high correlation (Figure 18). However, calculated $\delta^{18}O$ summertime temperature maxima do not show the same fullness of temperate range as the calculated $\delta^{18}O$ wintertime minima in an annual cycle. As a consequence, temperature calculations based on $\delta^{18}O$ measurements of coral skeletal material accreted during wintertime are judged to be more accurate temperature approximations than those calculated from skeletal material accreted during summertime months at the sampling resolution utilized in this study. The higher

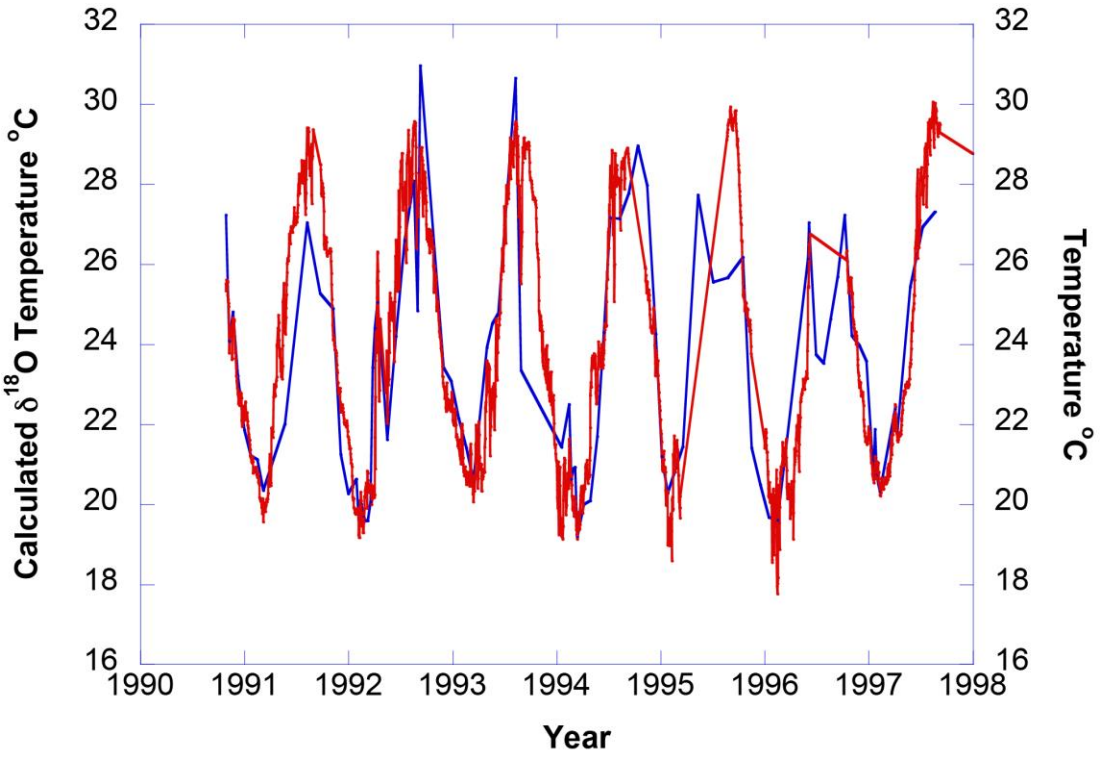

Figure 18. Time series of *M. faveolata* $\delta^{18}O$ derived temperature (Blue) and Flower Garden Banks *in situ* instrumental temperature from 1990 to 1998 (Red). Note that $\delta^{18}O$ temperatures match instrumental temperatures better for winter months than for summer months due to sampling resolution.

accuracy of calculated temperatures from wintertime $\delta^{18}O$ is due to the higher sampling resolution provided by sampling from portions of the coral with higher extension rates. More samples per unit time are collected from faster growing winter density bands resulting in less muting of the isotope signal due to sample averaging.

Increased calcification rates in coral skeletons have long been linked to stable isotope depletions [*McConnaughey*, 1989a,b] and since coral skeletal density is an indirect method of measuring past calcification rates, inferences can be made about how calcification has affected the stable isotope record presented here. Coral skeletal density variations in Flower Gardens *M. faveolata* lag behind seasonal variations of $\delta^{13}C$ and $\delta^{18}O$ and coral skeletal density consistently displays highest density values during the late summer/early fall time period (Figures 13a,b). Interestingly annual coral density maxima coincide with abrupt fall-time depletion in Flower Gardens coral $\delta^{13}C$. Assuming that seasonal photosynthesis follows annual patterns of insolation (Figure 17) and that seawater DIC remains relatively constant at the Flower Garden Banks [*Wagner and Slowey*, 2011], it can then be assumed that abrupt fall-time $\delta^{13}C$ depletions at the Flower Garden Banks are modulated by kinetic disequilibria effects [*McConnaughey*, 1989a,b] during fall-time high calcification periods.

An analysis of annual extension for the Flower Gardens *M. faveolata* coral core selected for this study reveals a two-step extension regime over the period 1844-2005 (Figure 19). The coral extension record before 1957 averaged an annual extension rate of 8.6-mm/year; in contrast, growth rates after 1957 averaged 7.2-mm/year – an average decrease in extension of 1.4-mm /year over the last 56 years (Table 1). The minimal

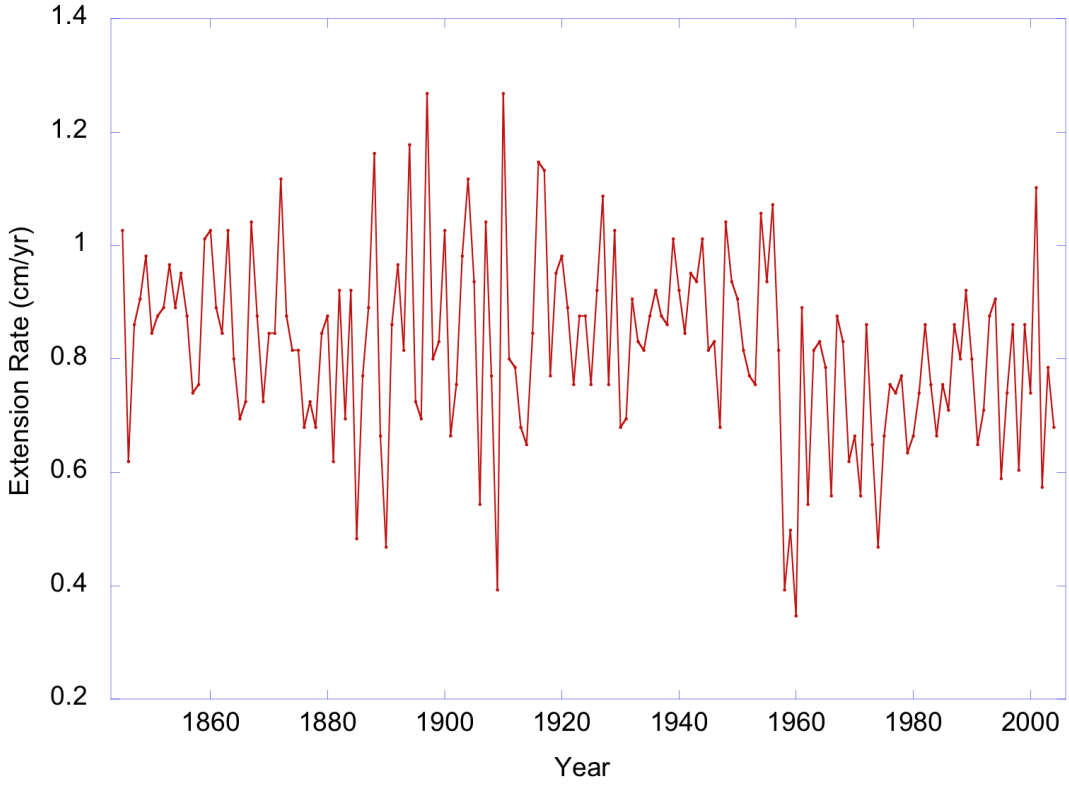

Figure 19. Time series of annual Flower Garden Banks *M. faveolata* coral extension. Note abrupt shift to slower extension rates after 1957.

observed growth year occurred in 1960 and approximately coincided with the described abrupt shift to slowed coral growth rates at the Flower Garden Banks. Similar to the findings presented here, *Slowey and Crowley* (1995) observed a large shift to slower growth rates in annual coral skeletal extension after the 1957/58 winter in 14 coral cores of both *M. faveolata* and *S. siderea*. Several justifications have been proposed for such a slowdown in extension rate including bank subsidence [*Rezak and Bright*, 1981] and more recently climatological variability associated with a wholesale shift to cooler winter temperatures in the Gulf of Mexico caused by the Pacific/North American Pattern after 1958 [*Slowey and Crowley*, 1995].

4.8. Long-Term $\delta^{13}C$ Trends

In our coral, we observe a net depletion of $\delta^{13}C$ over the time period 1843 to 2005, with a marked increase in the rate of depletion after 1960 (Figure 11). Could this pattern reflect the influence of a decrease of insolation on photosynthesis, or an increase of growth rate on biological fraction? Neither of these two possibilities seems plausible. Evidence suggests insolation was constant or increased slightly during the past two centuries [e.g., *Crowley*, 2000], which would tend to increase photosynthesis and coral $\delta^{13}C$ [*Weber and Woodhead*, 1970; *Goreau*, 1977]. The coral extension data presented here (Figure 19, Table 1) and in previous studies of Flower Garden Banks corals [*Slowey and Crowley*, 1995; and references therein] indicate that annual coral extension rates generally decrease after the winter of 1957, which would tend to increase coral $\delta^{13}C$ [*McConnaughey*, 1989a,b].

Since the onset of the industrial revolution, large amounts of ^{12}C-enriched CO_2 have been emitted into the atmosphere by the burning of fossil fuels and production of cement [e.g., *Crutzen and Stoermer*, 2000; *Houghton and Hackler*, 2002]. As a result, the concentration of atmospheric CO2 has risen from 280 to 395 ppm during the last two centuries [*Neftel*, 1985; *Keeling*, 2013] and the concentration of atmospheric CO_2 is now 40% greater than any other time during the last four hundred thousand years [*Petit et al*., 1999]. About a third of the released CO_2 has been taken up by seawater in the upper part of the ocean [*Sabine et al*., 2004]. Because fossil fuels tend to display depleted $\delta^{13}C$ values, the flux of this CO_2 into the ocean leads to a decrease in the $\delta^{13}C$ of the dissolved inorganic carbon (DIC) in seawater [e.g., *Nozaki et al*., 1978; *Druffel and Benavides*, 1986]. The trend of decreasing $\delta^{13}C$ in our coral record is interpreted as a reflection of the change in the $\delta^{13}C$ of DIC in the oceans a phenomenon otherwise known as the Suess Effect.

The $\delta^{13}C$ of the *M. faveolata* coral collected from the Flower Gardens Banks reveals a long-term negative trend over the last 160 years (Figure 11). The average $\delta^{13}C$ of the earliest ten year period (1843-1853 CE) of our record shows a value of -1.89‰. In contrast, the most recent ten year period (1995-2005 CE) has an average of -3.08‰ (Table 4). This result implies that $\delta^{13}C$ values in the Gulf of Mexico has become more negative by 1.2‰ over the last 162 years and is consistent with those found elsewhere in the oceans [e.g., *Nozaki et al*., 1978; *Druffel and Benavides*, 1986; *Swart*, 2010]. Interestingly, close inspection of the coral $\delta^{13}C$ record presented here shows that differences exist in rates of change of the annual winter minima and summer maxima of

$\delta^{13}C$ values: winter $\delta^{13}C$ values are depleting at more than two times the rate of summer values (Figure 9). To the best of our knowledge, this is the first time such an observation has been made.

As discussed by *Broecker* (1982), in a steady-state situation, the DIC of nutrient depleted warm surface waters in the oceans has a $\delta^{13}C$ value of ~2‰ due to the flux of "Redfield" organic matter from the surface to underlying waters. However, a steady state situation does not exist; there is an ongoing flux of ^{12}C enriched CO_2 from the atmosphere into warm surface ocean waters. In the Gulf of Mexico, greater wind velocities and surface ocean roughness [*DiMego et al*., 1976] and significantly cooler surface ocean temperatures (i.e., winters temperatures are ~12 °C cooler summer temperatures) during the winter drive a greater flux during that season, and there is consequently a greater impact on the $\delta^{13}C$ surface ocean DIC. This seasonal difference in the atmosphere to ocean fluxes of CO_2 is reflected by the seasonal difference in the long-term temporal trend of coral $\delta^{13}C$ at the Flower Garden Banks.

Superimposed on the centuries long trends of coral $\delta^{13}C$, interdecadal variations of $\delta^{13}C$ are also observed (Figure 11). Although it is tempting to attribute these variations to some cyclic environmental process that affects photosynthesis or coral calcification, we have not yet identified a potential process. It should be noted that *Swart* (2010) also observed similar long-term trends in the $\delta^{13}C$ records of 27 corals from the Atlantic, Pacific, and Indian Oceans. While many of these records displayed interdecadal variations, no consistent interdecadal pattern was recognized.

4.9. Speculations about 1902-1914 Depletion Event

A marked $\delta^{13}C$ depletion event is observable in our coral record during the 1902-14 time period after which $\delta^{13}C$ returns to previous to higher than previous values (Figure 11). The cause of the $\delta^{13}C$ depletion is unclear, but an examination of environmental and climatological data presents interesting possible scenarios. Previous studies have shown that $\delta^{13}C$ depletion in tests of calcareous organisms, including corals, can be associated, in part, with upwelling events or any other local shoaling event that introduces deeper, longer submerged water to more shallow environments [e.g., *Berger et al*., 1978, *Tudhope et al.*, 1996]. Such a case could be made with corals from the Flower Gardens based on coral $\delta^{13}C$ data. Similar to $\delta^{13}C$, $\Delta^{14}C$ also becomes more depleted with increasing water depth in the open ocean. However, because $\Delta^{14}C$ is a radiogenic isotope, its depletion is related only to age and therefore is useful as an absolute proxy for deep water shoaling events [e.g., *Goodkin et al*., 2012]. A recent study by *Wagner et al.* (2011) shows that corals representative of Gulf of Mexico and Caribbean seawater, which includes corals from the Flower Garden Banks, do not display a $\Delta^{14}C$ depletion. Therefore, we do not favor deep water shoaling as a cause of the 1902-14 $\delta^{13}C$ depletion event due to the lack of $\Delta^{14}C$ evidence.

Corals have long been known to be sensitive recorders of volcanic eruption events [e.g., *Gagan et al.*, 1995, *Crowley et al.*, 1997]. Carbon and oxygen isotopes as well as growth bands leave behind noticeable signals due to volcanically caused environmental stress. The onset of the $\delta^{13}C$ depletion event recorded in our Flower Gardens *M. faveolata* coral is in remarkable synchronicity with some of the most

powerful volcanic events that have occurred on the North American Continent in the last century (Figures 20a-d). 1902 marked the most violent volcanic year in recorded Caribbean history. The Santa Maria, Guatemala eruption is regarded as one of the five largest volcanic eruptions to occur in the last 300 years [*Williams and Self*, 1983]. Furthermore, the 1902 Mount Pelee eruption, on the island of Martinique is considered the worst volcanic disaster of the 20th century leveling the city of *St. Pierre* with a massive pyroclastic flow [*Lacroix*, 1904]. La Soufriere, located on the island of St. Vincent and the Grenadines is still considered an active volcano, although its most violent episode occurred in 1902, just hours before the eruption on Mount Pelee [*Anderson and Flett*, 1903]. In conjunction with these documented eruptions, our coral isotope record indicates a longer than normal winter following these May and October eruptions (Figure 20b). Oxygen isotopes indicate that the summer of 1903 was much shorter than the summers of 1902 and 1904 and was also cooler. The winter of 1903/1904 was also very long and cool. For the years following the extreme volcanically active year of 1902, $\delta^{13}C$ continues to deplete at a more accelerated rate than the years previous. In contrast, $\delta^{18}O$ indicates overall warming between 1902 and 1907 with the caveat of the 1902/1903, 1903/1904, and 1905/1906 winters being unusually cool. Following the 1902 to 1907 warming period, the time period from 1908 to 1914 indicate a transition to cooling with more mild summers being a defining characteristic. Carbon isotopes display their most negative values of the 1902-1914 time-period between the summer of 1912 to the summer of 1914. This period precisely follows the 1912 eruption

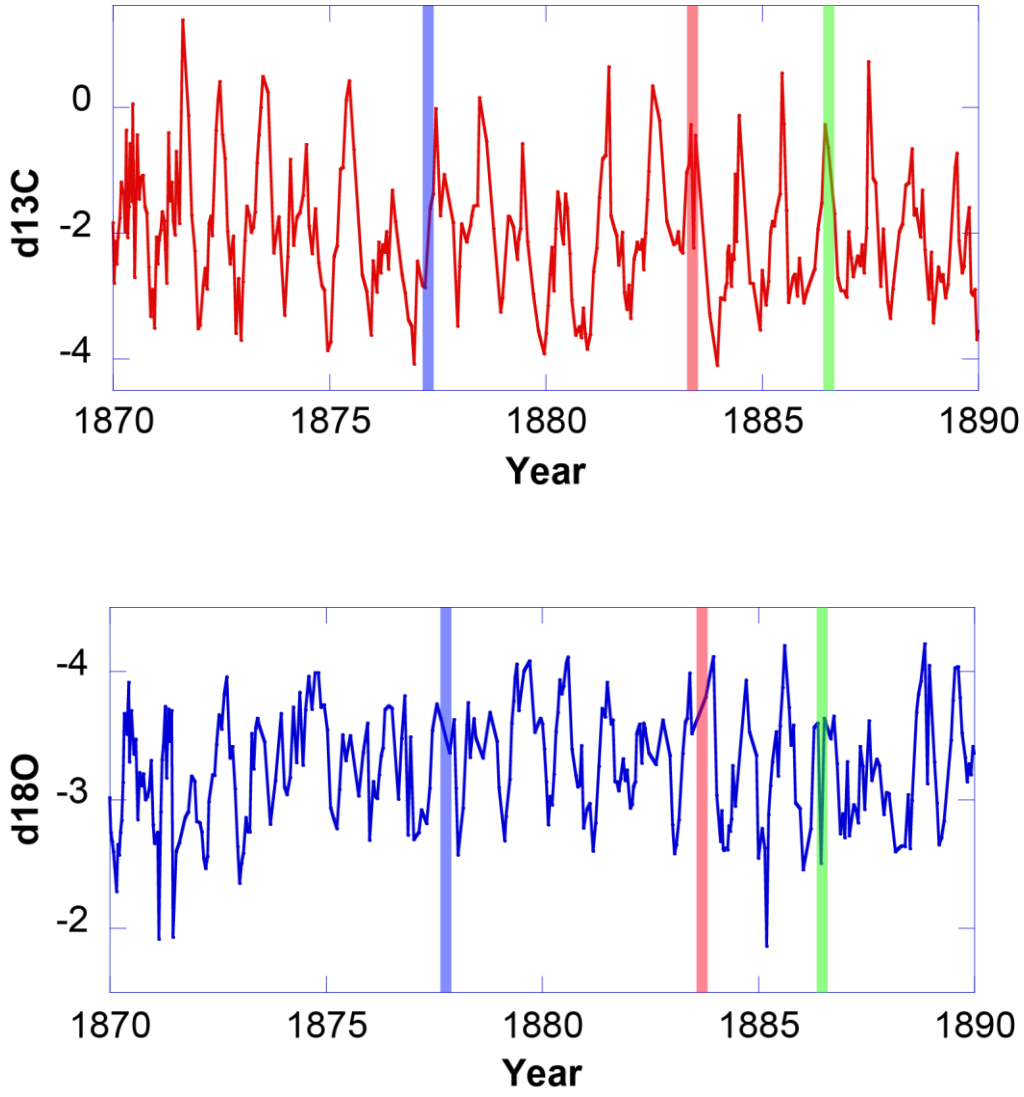

Figure 20a. Volcanic events Cotopaxi, Ecuador, 1877 (Blue); Krakatau, Indonesia, 1883 (Red); Tarawera, New Zealand, 1886 (Green) and the response of Flower Gardens *M. faveolata* coral as recorded in its skeletal isotope record.

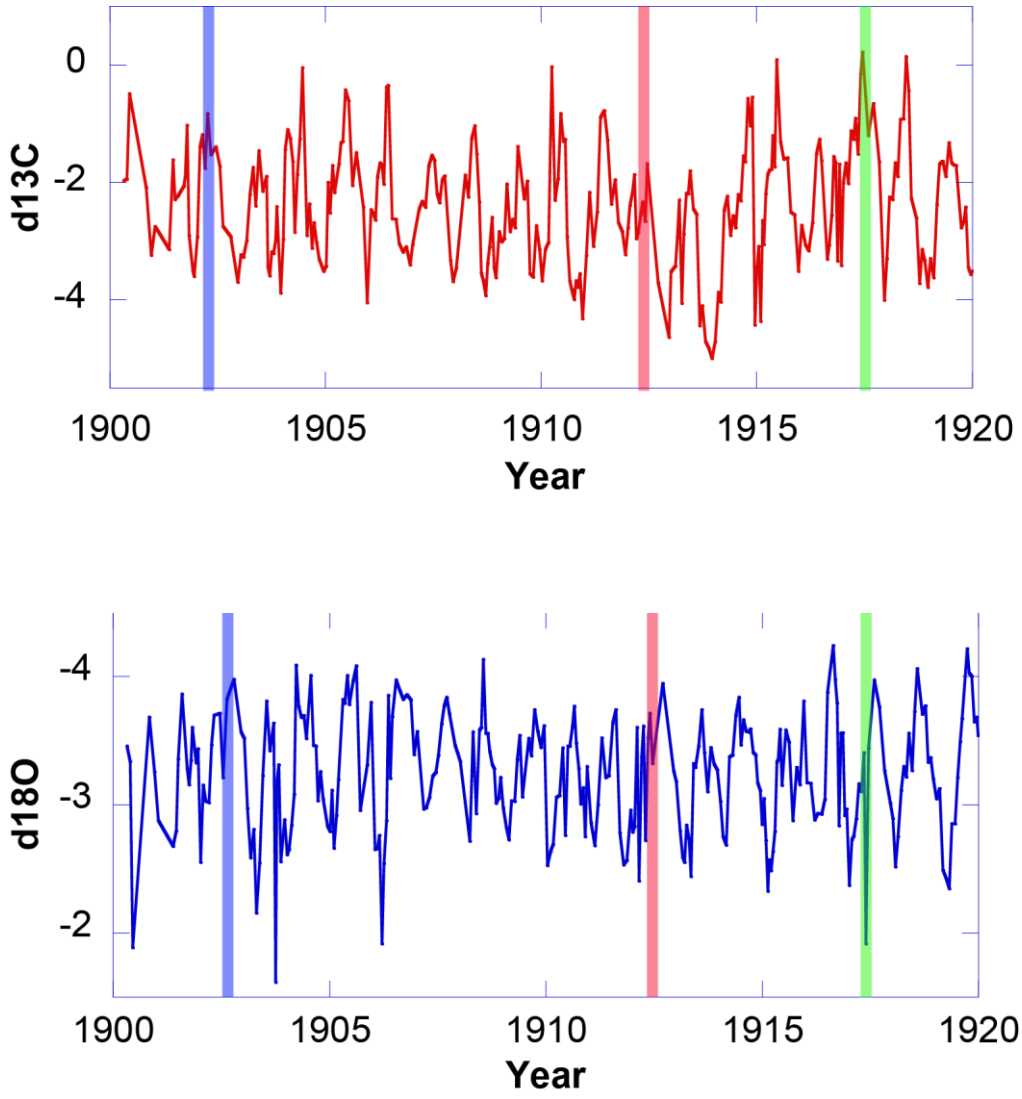

Figure 20b. Volcanic events Santa Maria, Guatemala, 1902 (Blue); Soufriere, Caribbean, 1902 (Blue); Pelee, Caribbean, 1902 (Blue); Novarupta at Katmai, Alaska, 1912 (Red); Agrigan, Marianas, 1917 (Green) and the response of Flower Gardens *M. faveolata* coral as recorded in its skeletal isotope record.

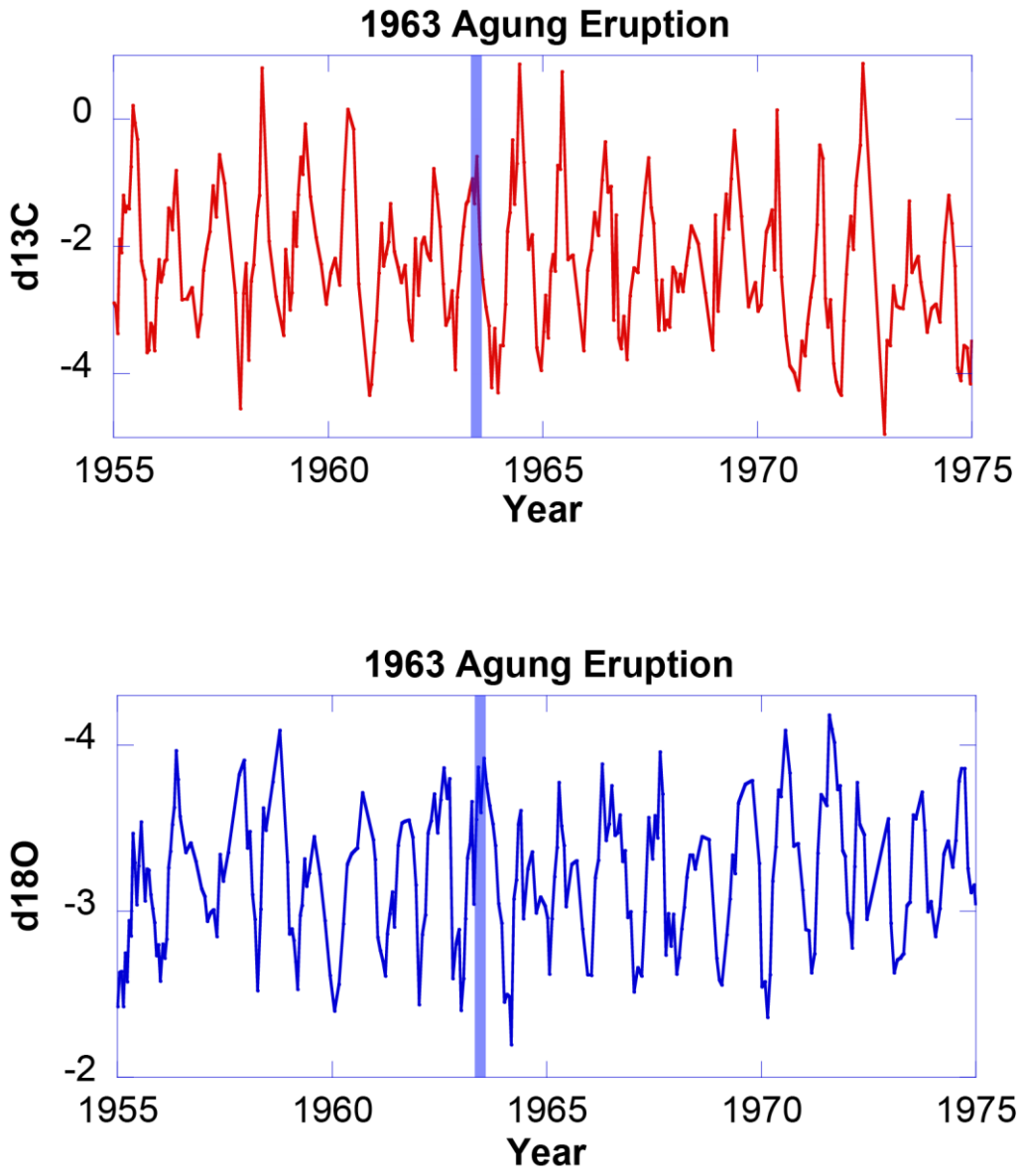

Figure 20c. Volcanic event Agung, Indonesia, 1963 (Blue) and the response of Flower Gardens *M. faveolata* coral as recorded in its skeletal isotope record.

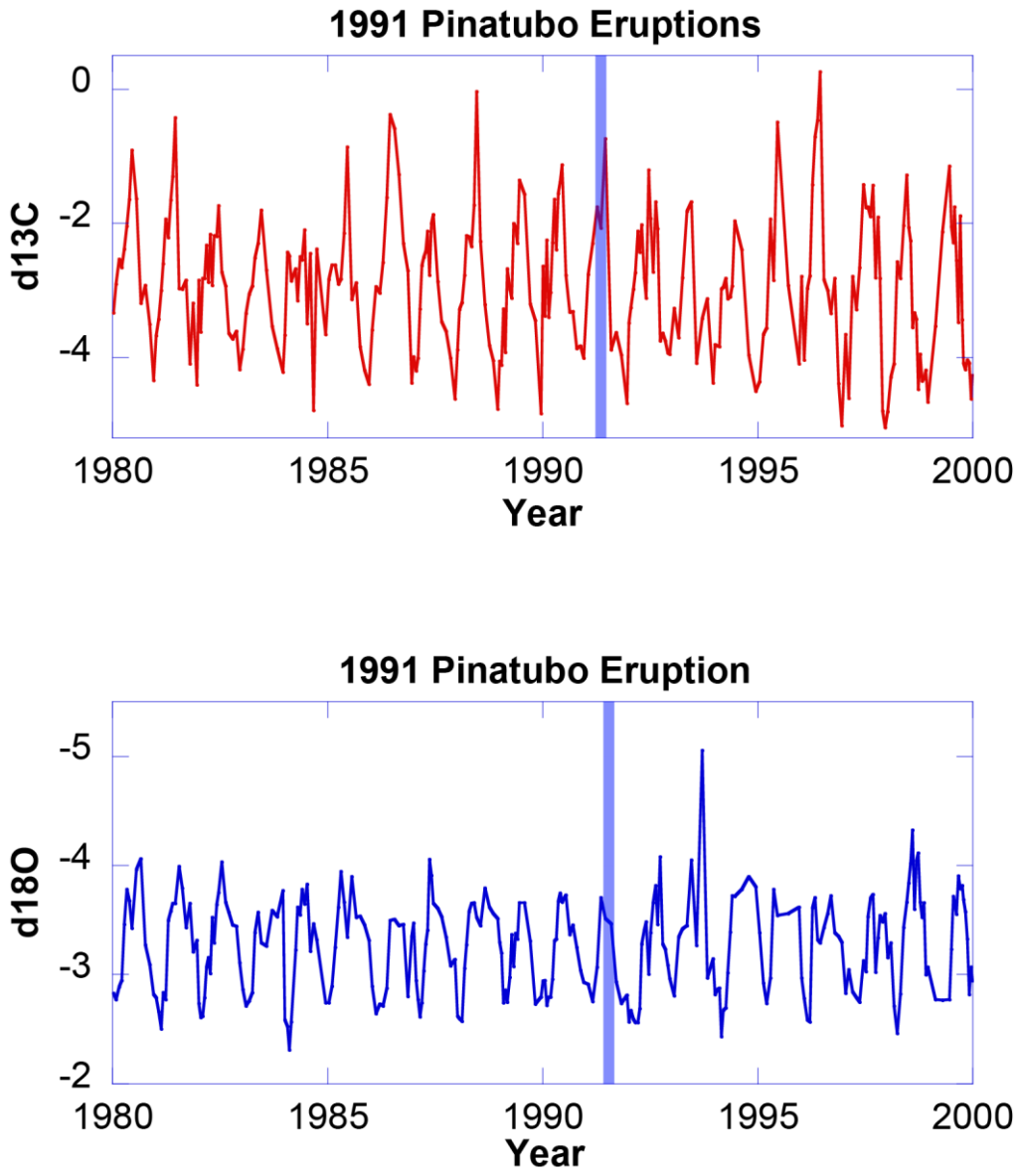

Figure 20d. Volcanic event Pinatubo, Philippines, 1991 (Blue) and the response of Flower Gardens *M. faveolata* coral as recorded in its skeletal isotope record.

of Novarupta at Katmai, Alaska, the largest eruption of the 20th century [*Hildreth*, 1987; *Hildreth and Fierstein*, 2012]. Winter $\delta^{13}C$ values fall to -5.0‰, their lowest values of the record to that point and more than 3.0‰ lower than average (Figure 20b). Oxygen and carbon isotopes both indicate that the winters of 1912/1913 and 1913/1914 are longer than normal. In turn, the summer of 1913 is shorter than normal and $\delta^{18}O$ indicates that temperatures are also depressed. Moreover, calculated extension rates of *M. faveolata* growth bands from the Flower Garden Banks show significant slowing of growth in 1902, 1912, 1913, and 1914 (Table 1). Each year corresponding to a year of an eruption or years following a major eruption. Furthermore, meteorological [*Sear et al*., 1987; *Bradley and Jones*, 1992; *Briffa et al*., 1998] and tree ring evidence from several sites located in North America and Europe show cooling and slowing of tree ring growth following the 1912 Novarupta at Katmai eruption [*LaMarche and Hirschboeck*, 1984; *Scuderi*, 1990; *Jones et al*., 1995; *Gindl*, 1999]. $\delta^{13}C$ evidence in tree rings from northern Europe also show a depletion event following the 1912 eruption [*McCarroll et al*., 2011]. Decreases in tree ring extension and $\delta^{13}C$ values are indicators of cooler ambient temperatures at the time of growth [*McCarroll et al*., 2011]. Therefore, it would follow that the similar growth band and $\delta^{13}C$ response observed in *M. faveolata* corals from the Flower Garden Banks would be expected. Especially considering that the North American jet stream flow comes in contact with the location of Katmai, Alaska and the Flower Garden Banks, thereby providing an efficient mode of transport for volcanic ash to the Flower Gardens region.

If major volcanic eruptions that have occurred on the North American continent and Caribbean affect the environmental conditions in the Gulf of Mexico and leave stable isotope and skeletal extension evidence in Flower Garden Corals, then other major global eruptions may have similar effects – if less extreme. Excluding the four major North American eruptions between 1902 and 1912 that were previously described, the timing of six major eruption events were analyzed in Flower Gardens *M. faveolata* stable isotope and skeletal extension data. The six major eruption events that we analyzed for included: Cotopaxi, Ecuador, 1877; Krakatau, Indonesia, 1883; Tarawera, N.Z., 1886; Agrigan, Marianas, 1917; Agung, Indonesia, 1963; and Pinatubo, Philippines, 1991 (Figures 20a,c,d). Timing of the eruption events were based on a chronology derived from published analyses of Antarctic ice records and later aggregated by *Crowley et al.,* 1997. Of the six major eruptions, the Flower Gardens *M. faveolata* $\delta^{18}O$ record presented here indicates that longer than normal winters followed thereafter with the exception of the 1917 Agrigan, Marianas eruption, which showed no isotopic or skeletal extension evidence following its occurrence (Figure 20b, Table 1). Furthermore, winters were also cooler than average following the 1883 Krakatoa, 1963 Agung, and 1991 Pinatubo eruptions (Figures 20a,c,d). Each of the three previously mentioned eruptions, have been determined to be the three greatest volcanic contributors to aerosol loading during the period recorded by Flower Gardens *M. faveolata* corals [*Crowley et al.,* 1997]. Carbon isotopes display longer than normal winter values following four of the six eruptions, with the exclusion of the 1877 Cotopaxi eruption and the 1917 Agrigan eruption (Figures 20a,b). Carbon isotope summer values were typically unaffected by volcanic

activity with the exception of the 1886 Tarawera eruption and the 1991 Pinatubo eruption, both of which displayed lower than normal summer $\delta^{13}C$ values (Figures 20a,d). Coral extension displayed slower rates of extension in times following four out of the six major eruptions, with the exception of the 1917 Agrigan and 1963 Agung eruptions (Figures 20b,c; Table 1).

The impact of the El Niño-Southern Oscillation on Flower Gardens corals are another important causal mechanism to consider for the 1902-1914 depletion event. At present, ENSO occurrences are thought to have a strong linkage with the Pacific/North American climate pattern [*Horel and Wallace*, 1981]. The PNA pattern is defined as coincident wintertime changes of atmospheric pressure at key field centers over North America [*Wallace and Gutzler*, 1981, *Yarnal and Diaz*, 1986, *Leathers et al*., 1991]. Positive phase PNA events coincide with changes in wintertime atmospheric pressure that redirects the path of the North American Jetstream to more southern reaches of the continent [*Yarnal and Diaz*, 1986; *Leathers et al*., 1991]. As a result, unusually cool arctic air is brought to the Flower Garden Banks during winter months [*Leathers et al*., 1991]. The PNA pattern, has strong implications for wintertime sea surface temperatures and precipitation in the Flower Gardens region. During an excited phase of the PNA pattern, winter temperatures at the Flower Garden Banks are lower and winter precipitation is higher than during non-PNA years [*Leathers et al*., 1991; *Rogers and Rohli*, 1991]. Therefore, coral density band extension rate and isotope composition at the Flower Garden Banks are faithful recorders of climatological variability related to ENSO and the PNA pattern [*Slowey and Crowley*, 1995]. Historical evidence indicates that a

high density of ENSO events occurred during the 1902-1914 Flower Gardens coral $\delta^{13}C$ depletion event. Data shows ENSO events occurred in 1902-1903, 1905-1906, 1911-1912, and 1914-1915. An examination of Flower Gardens *M. faveolata* $\delta^{18}O$ data shows that cooler than normal winter temperatures occurred during the winters of 1902/1903, 1903/1904, 1905-1906, 1911/1912, 1912/1913, and 1914/1915, (Figure 20b) each cool winter correlating to either a major regional volcanic event or ENSO climate anomaly. Additionally, the only strong La Niña event in the last 150 years also occurs in 1916, the effects of which are still unclear in the Flower Garden Banks region. In any case, $\delta^{13}C$ depletion during El Niño periods are further exacerbated by increased wintertime cloudiness associated with positive PNA events [*Leathers et al*., 1991] which suppresses photosynthesis.

5. CONCLUSIONS

In summary, examination of Flower Garden Banks *M. faveolata* isotopes and skeletal extension rates provide a high-resolution record of environmental change. Coral isotope and skeletal extension records were used to better understand fundamental aspects of coral isotope fractionation, how the surrounding environment affects coral physiological processes, and to reconstruct the past environmental conditions at the Flower Garden Banks. The major findings presented here shed new light on the behavior of carbon isotopes in coral skeletons in particular, as well as present a never before documented early 20th century volcanism-related environmental anomaly recorded in Flower Gardens *M. faveolata* geochemistry and skeletal extension rates.

A correlation of Flower Garden *M. faveolata* skeletal oxygen isotopes to *in situ* temperature measurements from the reef crest yielded a second order polynomial temperature relationship. The polynomial relationship is probably explained by extension rate related sampling bias or kinetic disequilibria isotope effects or some combination of the two. The temperature equation calibrated here is presently the only $\delta^{18}O$-temperature equation of its kind for *M. faveolata* at the Flower Garden Banks.

This study presents a new observed depth effect observed in Flower Garden *M. faveolata* corals. In contrast to previous studies that have primarily focused on near surface water corals (<5-m), the *M. faveolata* coral studied here was extracted from water depths of greater than 20 meters below the sea surface. Hourly *in situ* temperature measurements of seawater and an insolation model constructed for the Flower Garden Banks region exhibit a temporal offset as a result of the time required for seawater

temperature to respond to insolation changes (Figure 15). Interestingly, $\delta^{13}C$ and $\delta^{18}O$ display a near identical relationship as that of insolation and seawater temperature in Flower Garden *M. faveolata* coral material (Figures 14&15). Therefore, we conclude that *M. faveolata* carbon isotopes are not only recording the dampening of insolation as water depth increases, but also, the phase relationship between seawater temperature and insolation is captured in coral $\delta^{13}C$ and $\delta^{18}O$.

Photosynthesis and respiration are confirmed to be the primary control on $\delta^{13}C$ of the *M. faveolata* coral analyzed for this study. When the Flower Gardens *M. faveolata* coral $\delta^{13}C$ record is compared to a model-derived insolation record calibrated for the locality of the Flower Garden Banks, an extremely high correlation exists (Figure 17). Such a high correlation between $\delta^{13}C$ and insolation suggests that $\delta^{13}C$ could be used as a highly precise age identifier in corals when calibrated to annual solstices.

Carbon isotope annual maxima and minima calibrated to annual solstices at the Flower Garden Banks yields highly precise environmental reconstructions of past temperatures and insolation. The carbon isotope age calibration provides a more precise method of determining age than skeletal band counting and unlike $\delta^{18}O$; it does not require *in situ* reef crest measurements to ground truth results, as an insolation model is easily calculated with knowledge of latitude at the site of study.

Spawning periods are deemed an unlikely cause of annual $\delta^{13}C$ maxima in *M. faveolata* isotope records from the Flower Garden Banks. Spawning period calibration to $\delta^{13}C$ maxima yields $\delta^{18}O$ records that are offset to *in situ* instrumental temperature records by approximately two months (Table 5). Although we do not favor

coral spawning periods as a basis for determining age in *M. faveolata* isotope records or as the cause for $\delta^{13}C$ maxima, we do not dispute that spawning does at least have an effect on $\delta^{13}C$ values in *M. faveolata* skeletons.

A comparison of coral density variations, revealed by X-radiography and then quantified by ImageJ software, to coral $\delta^{13}C$ and $\delta^{18}O$ show a higher correlation exists between coral density and $\delta^{18}O$ seasonal cycles than with $\delta^{13}C$ seasonal cycles (Figures 13a,b). The observed coral density-$\delta^{18}O$ relationship at the Flower Garden Banks is in good agreement with previous studies that show coral extension is most likely related to annual seawater temperature variations and in turn, $\delta^{18}O$ [*Shinn,* 1966; *Highsmith,* 1979]. Furthermore, past calculated seawater temperatures from coral $\delta^{18}O$ indicate that winter values from coral $\delta^{18}O$ temperature calculations match *in situ* instrumentally recorded seawater temperatures better than any other time of year (Figure 18). A high wintertime $\delta^{18}O$-temperature correlation is explained by the higher rate of coral extension that occurs in winter months which results in a higher sampling rate and greater capability to resolve wintertime temperature changes.

A negative $\delta^{13}C$ excursion is observed in Flower Gardens *M. faveolata* coral that spans the approximate time period of 1902-1914 (Figure 11). The excursion occurs in conjunction with four of the largest volcanic eruptions of the last century, all of which occur near the Flower Gardens (in the Caribbean and Alaska). Furthermore, the timing of volcanic events: Cotopaxi, Ecuador, 1877; Krakatau, Indonesia, 1883; Tarawera, N.Z., 1886; Agrigan, Marianas, 1917; Agung, Indonesia, 1963; and Pinatubo, Philippines, 1991, were compared to the isotope and extension rate records of the Flower

Garden Coral presented here, and in most cases, isotopic and skeletal extension aberrations from the mean were detected in years of volcanic eruptions (Figure 11, Table 1).

The long-term $\delta^{13}C$ record reveals an overall negative trend for the past 162 years (Figure 11). Carbon isotope results from Flower Gardens *M. faveolata* indicates an average net $\delta^{13}C$ depletion of -1.19‰ over the whole record. We conclude that the $\delta^{13}C$ depletion is related to anthropogenic inputs of atmospheric CO_2 dating back to the industrial revolution. Furthermore, a long-term wintertime record of $\delta^{13}C$ shows a depletion rate that is more than twice that of the summertime record (Figure 9) resulting in greater annual $\delta^{13}C$ variability. The accelerated wintertime depletion rate is primarily related to low winter temperatures increasing the solubility of atmospheric CO_2 and thereby speeding up the process by which ocean carbon values deplete.

Coral isotope and extension records from the Flower Garden banks have provided a unique opportunity to study the past environmental change in the Northwest Gulf of Mexico. Future coral studies at the Flower Gardens have the potential to further our understanding about isotope processes in corals due to the truly exceptional environmental characteristics found there. The new findings and methods presented here may be of interest to the paleoceanographic community, as further coral studies in Gulf of Mexico will be necessary to better understand past oceanographic conditions in the region.

REFERENCES

Anderson, T. and J. S. Flett (1903), Report on the eruption of the Soufrière of St.Vincent in 1902 and on a visit to Montagne Pelée in Martinique. Pt. I: Royal Society Philosophical Transactions, p. 499-506, London, England.

Antonov, J. I., R. A. Locarnini, T. P. Boyer, A. V. Mishonov, and H. E. Garcia (2006), World Ocean Atlas 2005, vol. 2, p. 182, US Government Printing Office, Washington DC.

Barnes, D. J. and J. M. Lough (1993), On the nature and causes of density banding in massive coral skeletons, Journal of Experimental Biology and Ecology, 167, 91-108, doi: http://dx.doi.org/10.1016/0022-0981(93)90186-R

Berger, A. L. (1979), Long-term variations of daily insolation and quaternary climatic changes, Journal of the Atmospheric Sciences, 35, 2362-2367, doi: http://dx.doi.org/10.1175/1520-0469(1978)035%3C2362:LTVODI%3E2.0.CO;2.

Berger, W. H., L. Diester-Haass, and J. S. Killingsley (1978), Upwelling off north-west Africa: the Holocene decrease as seen in carbon isotopes and sedimentological indicators, Oceanologica Acta, 1, 3-7.

Bradley, R. S. and P. D. Jones (1992), Records of explosive volcanic eruptions over the last 500 years, in climate since A. D. 1500, Chapman Hall, pp. 606-622, New York, NY.

Briffa, K. R., P. D. Jones, F. H. Schweingruber, and T. J. Osborn (1998), Influence of volcanic eruptions on northern hemisphere summer temperature over the past 600 years, Nature, 393, 450-455, doi: 10.1038/30943.

Broecker, W. S., T. H. Peng, and Z. Beng, (1982), Tracers in the sea, Lamont-Doherty Geological Observatory, Columbia University.

Buddemeier, R. and R. Kinszie (1976), Coral growth, Oceanographic and Marine Annual Reviews, 14, 183-225.

Cobb, K. M., Charles, C. D., Cheng, H., and Edwards, R. L. (2003), El Niño/Southern Oscillation and tropical Pacific climate during the last millennium, Nature, 424, 271-276, doi: 10.1038/nature01779.

Cohen, A. L., G. D. Layne, and S. R. Hart (2001), Kinetic control of skeletal Sr/Ca in a symbiotic coral: Implications for the paleotemperature proxy, Paleoceanography, 16, 20-26, doi: 10.1029/1999PA000478.

Cole, J. E., R. G. Fairbanks, and G. T. Shen (1993), Recent variability in the Southern Oscillation: Isotopic results from a Tarawa atoll coral, Science, 260, 1790-1793, doi: 10.1126/science.260.5115.1790.

Crowley, T. J., T. M. Quinn, F. W. Taylor, C. Henin, and P. Joannot (1997), Evidence for a volcanic cooling signal in a 335-year coral record from New Caledonia, Paleoceanography, 12, 633-639, doi: 10.1029/97PA01348.

Crowley, T. J. (2000), Causes of climate change over the past 1000 years, Science, 289, 270-277, doi: 10.1126/science.289.5477.270.

Crutzen, P. J. and E. F. Stoermer (2000), IGBP Newsletter, 41, p. 12, Royal Swedish Academy of Sciences, Stockholm, Sweden.

DiMego, G. J., L. F. Bosart, and G. W. Endersen (1976), An examination of the frequency and mean conditions surrounding frontal incursions into the Gulf of Mexico and Caribbean Sea, Monthly Weather Review, 104, 709-718.

Dodge, R. E. and J. C. Lang (1983), Environmental correlates of hermatypic coral (*Montastrea annularis*) growth on the East Flower Gardens Bank, northwest Gulf of Mexico, Limnology and Oceanography, 28, 228-240.

Dodge, R. E. and J. Thomson (1974), The natural radiochemical and growth records in contemporary hermatypic corals from the Atlantic and Caribbean, Earth and Planetary Science Letters, 23, 313-322, doi: http://dx.doi.org/10.1016/0012-821X(74)90121-6.

Druffel, E. R. M. and L. M. Benavides (1986), Input of excess CO_2 to the surface ocean based on $^{13}C/^{12}C$ ratios in a banded Jamaican sclerosponge, Nature, 321, 58-61, doi:10.1038/321058a0.

Dunbar, R. B., and G. M. Wellington (1981), Stable isotopes in a branching coral monitor seasonal temperature variation, Nature, 1981, 453-455, doi: 10.1038/293453a0.

Dunbar, R. B., Wellington, G. M., Colgan, M. W., and Glynn, P. W. (1994), Eastern Pacific sea surface temperature since 1600 AD: The $\delta^{18}O$ record of climate variability in Galapagos corals. Paleoceanography, 9, 291-315, doi: 10.1029/93PA03501.

Erez, J. (1978), Vital effect on stable-isotope composition seen in foraminifera and coral skeletons, Nature, 273, 199-202, doi: 10.1038/273199a0.

Erhardt, R. D. (1990), Reconstructed annual minimum temperatures of the gulf states, 1799-1988, Journal of Climate, 3, 678-684, doi: http://adsabs.harvard.edu/cgi-bin/nph-abs_connect?fforward=http://dx.doi.org/10.1175/1520-0442(1990)003%3C0678:RAMTFT%3E2.0.CO;2.

Fairbanks, R. and R. Dodge (1979), Annual periodicity of the 18O/16O and 13C/12C ratios in the coral *Montastrea annularis*, Geochimica et Cosmochimica Acta, 43, 1009-1020, doi: http://dx.doi.org/10.1016/0016-7037(79)90090-5.

Gagan, M. K. and A. R. Chivas (1995), Oxygen isotopes in western Australian coral reveal Pinatubo aerosol-induced cooling in the Western Pacific Warm Pool, Geophysical Research Letters, 22, 1069-1072, doi: 10.1029/95GL00607.

Gagan, M. K., A. R. Chivas, and P. J. Isdale (1996), Timing coral-based climatic histories using ^{13}C enrichments driven by synchronized spawning, Geology, 24, (11), 1009-1012, doi: 10.1130/0091-7613(1996)024<1009:TCBCHU>2.3.CO;2.

Gindl, W. (1999), Climatic significance of light rings in timberline spruce, *Picea abies*, Austrian Alps, Arctic, Antarctic, and Alpine Research, 31, 242-246.

Giry, C., T. Felis, M. Kolling, W. Wei, G. Lohmann, and S. Scheffers (2013), Controls of Caribbean surface hydrology during the mid- to late Holocene: Insights from monthly resolved coral records, Climate of the Past, 9, 841-858.

Gittings, S. R., G. S. Boland, K. J. P. Deslarzes, C. L. Combs, B. S. Holland, and T. J. Bright (1992), Mass spawning and reproductive viability of reef corals at the East Flower Garden Bank, Northwest Gulf of Mexico, Bulletin of Marine Science, 51, 420-428.

Gledhill, D., R. Wanninkhof, F. J. Millero, and M. Eakin (2008), Ocean acidification of the greater Caribbean region 1996-2006, Journal Geophysical Research, 113, C10031, doi:10.1029/2007JC004629.

Goodkin, N. F., E. R. M. Druffel, K. A. Hughen, and S. C. Doney (2012), Two centuries of limited variability in subtropical North Atlantic thermocline ventilation, Nature Communications, 3, 1-6, doi:10.1038/ncomms1811.

Goreau, T. J. (1977), Coral skeletal chemistry: physiological and environmental regulation of stable isotopes and trace metals in *Montastrea annularis*, Proceedings of the Royal Society: Biological Sciences, 196, 291-315, doi: 10.1098/rspb.1977.0042.

Grottoli, A. G. and G. M. Wellington (1999), Effect of light and zooplankton on skeletal $\delta^{13}C$ values in the eastern Pacific corals *Pavona clavus* and *Pavona gigantea*, Coral Reefs, 18, 29-41.

Hagman, D. K. and S. R. Gittings (1992), Coral bleaching on high latitude reefs at the Flower Garden Banks, NW Gulf of Mexico, Proceedings of the 7th International Coral Reef Symposium, Guam, 1, 38-43.

Hansen, J. E. (1971), Multiple scattering of polarized light in planetary atmospheres. Part II. Sunlight reflected by terrestrial water clouds, Journal of Atmospheric Sciences, 28, 1400-1426.

Hildreth, W. (1987), New perspectives on the eruption of 1912 in the Valley of Ten Thousand Smokes, Katmai National Park, Alaska, Bulletin of Volcanology, 49, 680-693, doi: 10.1007/BF01080359.

Hildreth, W. and J. Fierstein, The Novarupta-Katmai eruption of 1912—largest eruption of the twentieth century: Centennial perspectives, Professional Paper 1791, 1-12, 2012.

Houghton, R. A. and J. L. Hackler, in Trends: A compendium of data on global change (Carbon Dioxide Information Analysis Center, Oak Ridge National Laboratory, TN, 2002), http://cdiac.esd.ornl.gov/trends/landus/houghton/houghton.html

Horel, J. D. and J. M. Wallace (1981), Planetary-scale atmospheric phenomena associated with the Southern Oscillation, American Meteorological Society, 109, 813-829.

Howell, P., N. Pisias, J. Ballance, J. Baughman, and L. Ochs (2006) ARAND time-series analysis software. Brown University, Providence RI.

Hudson, J. H., E. A. Shinn, R. B. Halley, and B. Lidz (1976), Sclerochronology: a tool for interpreting past environments, Geology, 4, 361-364, doi: 10.1130/0091-7613(1976)4<361:SATFIP>2.0.CO;2.

Hudson, J. H.; and D. M. Robbin (1980), Chapter 17 Effects of drilling mud on the growth rate of the reef-building coral, *Montastrea annularis*, Elsevier Oceanography Series, 27, 455-470.

Humphris, C. C. (1979), Salt movement on continental slope, northern Gulf of Mexico, AAPG Bulletin, 63, 782-798.

Jones, P. D., K. R. Briffa, and F. H. Schweingruber (1995), Tree-ring evidence of the widespread effects of explosive volcanic eruptions, Geophysical Research Letters, 22, 1333-1336, doi: 10.1029/94GL03113.

Knutson, D. W. and S. V. Smith (1972), Coral chronometers: Seasonal growth bands in reef corals, Science, 177, 270-272, doi: 10.1126/science.177.4045.270.

Lacroix, A. (1904), La Montagne Pelée et ses eruptions, Académie des sciences, Paris, France.

Lamarche, V. C. and K. K. Hirschboeck (1984), Frost rings in trees as records of major volcanic eruptions, Nature, 307, 1-3.

Land, L. S., J. C. Lang, and B. N. Smith (1975), Preliminary observations on the carbon isotopic composition of some reef coral tissues and symbiotic zooxanthellae, Limnology and Oceanography, 283-287.

Land, L. S., J. C. Lang, and D. J. Barnes (1977), On the stable carbon and oxygen isotopic composition of some shallow water, ahermatypic, scleractinian coral skeletons, Geochimica et Cosmochimica Acta, 41, 169-172, doi: http://dx.doi.org/10.1016/0016-7037(77)90197-1.

Leathers, D. J., B. Yarnal, and M. A. Palecki (1991), The Pacific/North American teleconnection pattern and the United States climate. Part I: Regional temperature and precipitation associations, Journal of Climate, 4, 517-528, doi: http://dx.doi.org/10.1175/1520-0442(1991)004%3C0517:TPATPA%3E2.0.CO;2.

Leder, J. J., P. K. Swart, A. M. Szmant, and R. E. Dodge, The origin of variations in the isotopic record of scleractinian corals: I. Oxygen, 60, 2857-2870, doi: http://dx.doi.org/10.1016/0016-7037(96)00118-4.

Levert Jr, C. F., and H. C. Ferguson Jr. (1969), Geology of West Flower Garden Bank, northwest Gulf of Mexico, AAPG Bulletin, 53, 2039-2039.

Linsley, B. K., L. Ren, R. B. Dunbar, and S. S. Howe (2000), El Niño-Southern Oscillation (ENSO) and decadal-scale climate variability at 10^{o}N in the eastern Pacific from 1893 to 1994: A coral –based reconstruction from Clipperton Atoll, Paleoceanography, 15, 322-335, doi: 10.1029/1999PA000428.

McCarroll, D., M. Tuovinen, R. Campbell, M. Gagen, H. Grudd, R. Jalkanen, N. J. Loader, and I. Robertson (2011), A critical evaluation of multi-proxy dendroclimatology in northern Finland, 26, 7-14, doi: 10.1002/jqs.1408.

McConnaughey, T. A. (1989), ^{13}C and ^{18}O isotopic disequilibrium in biological carbonates: I. Patterns, Geochimica et Cosmochimica Acta, 53, 151-162, doi: http://dx.doi.org/10.1016/0016-7037(89)90282-2.

McConnaughey, T. A. (1989), 13C and 18O isotopic disequilibrium in biological carbonates: II. In vitro simulation of kinetic isotope effects, 53, 163-171, doi: http://dx.doi.org/10.1016/0016-7037(89)90283-4.

McConnaughey, T. A., J. Burdett, J. F. Whelan, and C. K. Paull (1997), Carbon isotopes in biological carbonates: Respiration and photosynthesis, Geochimica et Cosmochimica Acta, 61, 611-622, doi: http://dx.doi.org/10.1016/S0016-7037(96)00361-4.

Moyer, R. P. and A. G. Grottoli (2011), Coral skeletal carbon isotopes ($\delta^{13}C$ and $\Delta^{14}C$) record the delivery of terrestrial carbon to the coastal waters of Puerto Rico, Coral Reefs, 30, 791-802, doi: 10.1007/s00338-011-0758-y.

Nowlin, W. D. and C. A. Parker (1974), Effects of a cold-air outbreak on shelf waters of the Gulf of Mexico, Journal of Physical Oceanography, 4, 467-486.

Nozaki, Y., D. M. Rye, K. K. Turekian, and R. E. Dodge (1978), A 200 year record of Carbon-13 and Carbon-14 variations in a Bermuda coral, Geophysical Research Letters, 5, 825-828, doi: 10.1029/GL005i010p00825.

Ostermann, D. R. and W. B. Curry (2000), Calibration of stable isotopic data: An enriched $\delta^{18}O$ standard used for source gas mixing detection and correction, Paleoceanography, 15, 353-360, doi: 10.1029/1999PA000411.

Patzold, J. (1984), Growth rhythms recorded in stable isotopes and density bands in the reef coral *Porites lobata* (Cebu, Philippines), Coral Reefs, 3, 87-90.

Patzold, J. (1992), Variation of stable oxygen and carbon isotopic fractionation within the skeletal elements of reef building corals from Bermuda, Proceedings of the 7th International Coral Reef Symposium, Guam, 1, 196-200.

Peel, F. J., C. J. Travis, and J. R. Hossack (1995), Genetic structural provinces and salt tectonics of the Cenozoic offshore US Gulf of Mexico; a preliminary analysis, Salt Tectonics, AAPG Memoir, 65, 153-175.

Reed, R. K. (1977), On Estimating Insolation over the Ocean, Journal of Physical Oceanography, 7, 482-485, doi: http://dx.doi.org/10.1175/1520-0485(1977)007%3C0482:OEIOTO%3E2.0.CO;2.

Rezak, R., T. J. Bright, and W. McGrail (1985), Reefs and banks of the northern Gulf of Mexico, pp. 259, Wiley-Interscience, New York.

Rogers, J. and R. Rohli (1991), Florida citrus freezes and polar anticyclones in the Great Plains, Journal of Climate, 4, 1103-1113, doi: http://dx.doi.org/10.1175/1520-0442(1991)004%3C1103:FCFAPA%3E2.0.CO;2.

Sabine, C. L., R.A. Feely, N. Gruber, R. M. Key, K. Lee, J. L. Bullister, R. Wanninkhof, C. S. Wong, D. W. R. Wallace, B. Tilbrook, F. J. Millero, T. H. Peng, A. Kozyr, T. Ono, and A. F. Rios (2004), The oceanic sink for anthropogenic CO_2, Science, 305, 367-371, doi: 10.1126/science.1097403.

Schneider, C. A., W. S. Rasband, and K. W. Eliceiri, (2012) NIH Image to ImageJ: 25 years of image analysis, Nature Methods 9, 671-675.

Scuderi, L. A. (1990), Tree-ring evidence for climatically effective volcanic eruptions, Quaternary Research, 34, 67-85, doi: http://dx.doi.org/10.1016/0033-5894(90)90073-T.

Sear, C. B., P. M. Kelly, P. D. Jones, and C. M. Goodess (1987), Global surface-temperature responses to major volcanic eruptions, Nature, 330, 365-367, doi: 10.1038/330365a0.

Shen, G. T., J. E. Cole, D. W. Lea, L. J. Linn, T. A. McConnaughey, and R. G. Fairbanks (1992), Surface ocean variability at Galapagos from 1936-1982: Calibration of geochemical tracers in corals, Paleoceanography, 7, 563-588, doi: 10.1029/92PA01825.

Shinn, E. A. (1966), Coral growth-rate, an environmental indicator, Journal of Paleontology, 40, 233-241.

Slowey, N. and T. Crowley (1995) Interdecadal variability of Northern Hemisphere circulation recorded by Gulf of Mexico corals, Geophysical Research Letters, 22, 2345-2348.

Stephans, C. L., T. M. Quinn, F. W. Taylor, and T. Corrège (2004). Assessing the reproducibility of coral-based climate records. Geophysical research letters, 31, doi: 10.1029/2004GL020343.

Swart, P. K. (1983), Carbon and oxygen isotope fractionation in scleractinian corals: a review, Earth-Science Reviews, 19, 51-80, doi: http://dx.doi.org/10.1016/0012-8252(83)90076-4.

Swart, P. K., J. J. Leder, A. M. Szmant, and R. E. Dodge (1996), The origin of variations in the isotopic record of scleractinian corals: II. Carbon, Geochimica et Cosmochimica Acta, 60, 2871-2885, doi: http://dx.doi.org/10.1016/0016-7037(96)00118-4.

Swart, P. K., G. F. Healy, R. E. Dodge, P. Kramer, J. H. Hudson, R. B. Halley, and M. B. Roblee (1996), The stable oxygen and carbon isotopic record from a coral growing in Florida Bay: a 160 year record of climatic and anthropogenic influence, Palaeogeography, Palaeoclimatology, Palaeoecology, 123, 219-237, doi: http://dx.doi.org/10.1016/0031-0182(95)00078-X.

Swart, P. K., L. Greer, B. E. Rosenheim, C. Moses, A. Winter, K. Helmle, and R. E. Dodge (2010), ^{13}C Suess effect in scleractinian corals mirror changes in the anthropogenic CO2 inventory of the surface oceans, Geophysical Research Letters, 37, 1-5, doi: 10.1029/2009GL041397.

Szmant, A. M. (1986), Sexual reproduction by the Caribbean reef corals: Coral Reefs, 5, 43-54.

Tudhope, A. W., G. B. Shimmield, C. P. Chilcott, M. Jebb, A. E. Fallick, and A. N. Dalgleish (1995), Recent changes in climate in the far western equatorial Pacific and their relationship to the Southern Oscillation; oxygen isotope records from massive corals, Papua New Guinea, Earth and Planetary Science Letters, 136, 575-590, doi: http://dx.doi.org/10.1016/0012-821X(95)00156-7.

Tudhope, A. W., D. W., Lea, G. B. Shimmield, C. P. Chilcott, and S. Head (1996), Monsoon climate and Arabian coastal upwelling recorded in massive corals from southern Oman, Palaios, 11, 347-361.

Vize, P. D., J. A. Embesi, M. Nickell, D. P. Brown, and D. K. Hagman (2005), Tight temporal consistency of coral mass spawning at the Flower Garden Banks, Gulf of Mexico, from 1997–2003, Gulf of Mexico Science, 1, 107-114.

Wagner, A. J. and N. C. Slowey (2011), Oxygen isotopes in seawater from the Texas-Louisiana Shelf, Bulletin of Marine Science, 87, 1–12, doi: http://dx.doi.org/10.5343/bms.2010.1004.

Wagner, A. J., T.P Guilderson, N. C. Slowey, and J. E. Cole (2011), Pre-bomb surface water radiocarbon of the Gulf of Mexico and Caribbean as recorded in hermatypic corals, Radiocarbon, 51, 947-954.

Wallace, J. M. and D. S. Gutzler (1981), Teleconnections in the geopotential height field during the Northern Hemisphere winter, Monthly Weather Review, 109, 784-812, doi: http://dx.doi.org/10.1175/1520-0493(1981)109%3C0784:TITGHF%3E2.0.CO;2.

Watanabe, T., A. Winter, T. Oba, R. Anzai, and H. Ishioroshi (2002). Evaluation of the fidelity of isotope records as an environmental proxy in the coral *Montastraea*. Coral Reefs, 21, 169-178, doi: 10.1007/s00338-002-0218-9.

Weber, J. N. and P. M. J. Woodhead (1970), Carbon and oxygen isotope fractionation in the skeletal carbonate of reef-building corals, Chemical Geology, 6, 93-117, doi: http://dx.doi.org/10.1016/0009-2541(70)90009-4.

Weber, J. N. and P. M. J. Woodhead (1972), Temperature dependence of Oxygen-18 concentration in reef coral carbonates, Journal of Geophysical Research, 77, 463-473, doi: 10.1029/JC077i003p00463.

Weil, S. M., R. W. Buddemeier, S. V. Smith, and P. M. Kroopnick (1981). The stable isotopic composition of coral skeletons: control by environmental variables. Geochimica et Cosmochimica Acta, 45, 1147-1153, doi: http://dx.doi.org/10.1016/0016-7037(81)90138-1.

Wellington, G. M. and P. W. Glynn (1983), Environmental influences on skeletal banding in eastern Pacific (Panama) corals, Coral Reefs, 1, 215-222.

Williams, S. N. and S. Self (1983), The October 1902 plinian eruption of Santa Maria Volcano, Guatemala, Journal of Volcanology and Geothermal Research, 16, 33-56, doi: http://dx.doi.org/10.1016/0377-0273(83)90083-5.

Yarnal, B. and H. F. Diaz (1986), Relationships between extremes of the Southern Oscillation and the winter climate of the Anglo-American Pacific Coast, Journal of Climatology, 6, 197-219, 10.1002/joc.3370060208.